

RESEARCH ARTICLE

A High Temperature-Dependent Mitochondrial Lipase EXTRA GLUME1 Promotes Floral Phenotypic Robustness against Temperature Fluctuation in Rice (*Oryza sativa* L.)

Biya Zhang^{1,2*}, Shaohuan Wu^{2,3*}, Yu'e Zhang¹, Ting Xu¹, Feifei Guo^{1,2}, Huashan Tang^{1,2}, Xiang Li^{1,2}, Pengfei Wang^{1,2}, Wenfeng Qian³, Yongbiao Xue^{1,4,5*}

1 State Key Laboratory of Molecular Developmental Biology, Institute of Genetics and Developmental Biology, Chinese Academy of Sciences and National Center for Plant Gene Research, Beijing, the People's Republic of China, **2** University of Chinese Academy of Sciences, Beijing, the People's Republic of China, **3** State Key Laboratory of Plant Genomics, Institute of Genetics and Developmental Biology, Chinese Academy of Sciences, Beijing, the People's Republic of China, **4** Beijing Institute of Genomics, Chinese Academy of Sciences, Beijing, the People's Republic of China, **5** Collaborative Innovation Center for Genetics and Development, Fudan University, Shanghai, the People's Republic of China

* These authors contributed equally to this work.

* ybxue@genetics.ac.cn



CrossMark
click for updates

OPEN ACCESS

Citation: Zhang B, Wu S, Zhang Y, Xu T, Guo F, Tang H, et al. (2016) A High Temperature-Dependent Mitochondrial Lipase EXTRA GLUME1 Promotes Floral Phenotypic Robustness against Temperature Fluctuation in Rice (*Oryza sativa* L.). PLoS Genet 12(7): e1006152. doi:10.1371/journal.pgen.1006152

Editor: Hao Yu, National University of Singapore and Temasek Life Sciences Laboratory, SINGAPORE

Received: January 6, 2016

Accepted: June 8, 2016

Published: July 1, 2016

Copyright: © 2016 Zhang et al. This is an open access article distributed under the terms of the [Creative Commons Attribution License](#), which permits unrestricted use, distribution, and reproduction in any medium, provided the original author and source are credited.

Data Availability Statement: All relevant data are within the paper and its Supporting Information files.

Funding: This work was supported by grants from Ministry of Science and Technology (2013CBA01402), Strategic Program of Chinese Academy of Sciences (XDA08010205) and National Natural Science Foundation of China (31221063). The funders had no role in study design, data collection and analysis, decision to publish, or preparation of the manuscript.

Abstract

The sessile plants have evolved diverse intrinsic mechanisms to control their proper development under variable environments. In contrast to plastic vegetative development, reproductive traits like floral identity often show phenotypic robustness against environmental variations. However, it remains obscure about the molecular basis of this phenotypic robustness. In this study, we found that *eg1* (*extra glume1*) mutants of rice (*Oryza sativa* L.) showed floral phenotypic variations in different growth locations resulting in a breakdown of floral identity robustness. Physiological and biochemical analyses showed that *EG1* encodes a predominantly mitochondria-localized functional lipase and functions in a high temperature-dependent manner. Furthermore, we found that numerous environmentally responsive genes including many floral identity genes are transcriptionally repressed in *eg1* mutants and *OsMADS1*, *OsMADS6* and *Osg1* genetically act downstream of *EG1* to maintain floral robustness. Collectively, our results demonstrate that *EG1* promotes floral robustness against temperature fluctuation by safeguarding the expression of floral identity genes through a high temperature-dependent mitochondrial lipid pathway and uncovers a novel mechanistic insight into floral developmental control.

Competing Interests: The authors have declared that no competing interests exist.

Author Summary

Various mechanisms have evolved to ensure proper organ formation under variable environments in order to complete one organism's life cycle. In angiosperms, vegetative and reproductive organs show a differential plastic development between varied environments, with a low plasticity or high robustness for flower formation, but little is known about its intrinsic mechanism. Here we report that gene *EG1* (*EXTRA GLUME1*) can enhance the floral robustness against temperature fluctuation in rice. *EG1* encodes a predominantly mitochondria-localized functional lipase and its loss of function disrupts floral development in a high temperature-dependent manner. In consistent, both *EG1* and its lipase activity are positively induced by high temperature. Transcriptomic and genetic analyses revealed that *EG1* functions upstream of several floral identity genes, eg, *OsMADS1*, *OsMADS6* and *OsG1*. Taken together, our results uncover a novel mitochondria-mediated lipid metabolic pathway to promote floral developmental robustness. Our findings may help to genetically improve floral traits of rice to maintain a stable yield when planted in different locations and/or under heat stress conditions.

Introduction

The sessile plants have evolved various exquisite adaptive strategies to cope with environmental changes [1,2]. Among them, phenotypic plasticity is the ability of a single genotype capable of producing different phenotypes in response to varying environments [3–6]. For an integral high fitness, morphologies of vegetative organs of a single plant, such as roots, leaves and stems, require a high phenotypic plasticity [7–10], whereas that of reproductive organs, such as flowers, fruits and seeds, are always associated with low plasticity also known as phenotypic robustness/stability [11–15]. Thus, plants must coordinate the developments of these organs.

Compared with progresses in understanding the molecular mechanisms of high phenotypic plasticity [10,16–19], very little is known about the molecular basis of phenotypic robustness [20,21]. Recent studies have shown that there are a group of specific genes regulating the degree of phenotypic plasticity and determining the reaction norm of a trait among various environments, which are termed plasticity genes [22–24]. However, most of the identified plasticity genes are high plasticity-associated [16,25–27], only few promote phenotypic robustness [28–30]. Members of *HSP90* (*HEAT SHOCK PROTEIN 90*) family, as central hubs of numerous biological pathways, are required for maintenance of phenotypic robustness in both animals and plants [28,31–34]. *MSH1* (MutS HOMOLOG1), a homolog of bacterial mismatch repair protein MutS, has been reported to repress the developmental plasticity of plant architecture, leaf morphology and flowering time in several dicot and monocot plants [29,35]. A nuclear protein *RPL1* (RICE PLASTICITY1) in rice also appears to promote the relatively stable plant architecture and panicle structure between different environments [30]. Despite these discoveries, we still know very little about the molecular mechanisms of phenotypic robustness, especially that of plant reproductive traits. In addition to the known epigenetics-dependent transcriptional regulation and hormone signaling [20,29–31,35], lipid homeostasis is also known to influence phenotypic robustness [36,37]. Coordinated regulations of cellular lipid homeostasis are crucial to organisms' adaptive robustness under severe temperatures [37–40]. Furthermore, lipid-related synthetases and lipases can also be regulated at transcriptional and posttranslational levels to influence lipid homeostasis [41,42]. Among them, mitochondria-associated lipid metabolism is key to the lipid homeostasis [43]. For instance, *Arabidopsis* seedlings with decreased cardiolipin in mitochondrial membrane are easier to turn yellow and

necrotic under extended darkness or heat due to a failure of mitochondrial morphogenesis, showing a lowered stability [41,44,45]. However, it remains unclear whether mitochondria also mediate the phenotypic robustness in plant reproductive organs.

Flower morphology, as a gold standard in plant taxonomy, has the most remarkable robustness within and between individuals of the same population [11,46], making it an ideal trait for studies on the molecular basis of phenotypic robustness against environmental fluctuation.

Nevertheless, so far no gene has been identified to regulate the phenotypic robustness of floral identity, although several environment-dependent floral mutants have been reported [47–52]. We previously found that a rice floral mutant *eg1* (*extra glume1*) exhibited a floral variation in different growth conditions [53], implying that *EG1* is likely involved in floral robustness.

Recent studies have shown that *EG1* encodes a putative lipase regulating rice floral identity and meristem determinacy [53]. It also functions in JA (jasmonic acid) biosynthesis to promote the expression of floral identity gene *OsMADS1* through an *EG2/OsJAZ1*, *OsCOIb* and *OsMYC2*-mediated JA signaling pathway [54], similar to its homologous genes *AtDAD1* (*DEFECTIVE IN ANOTHER DEHISCENCE1*) and *AtDGL* (*DONGLE*) in Arabidopsis [55,56]. In this study, we find that *EG1* is a predominantly mitochondria-localized functional lipase and promotes floral robustness against temperature fluctuation in a high temperature-dependent manner. Collectively, our results reveal a novel molecular mechanism underlying floral phenotypic robustness.

Results

eg1 shows high plasticity in floral identity through an interaction of genotype and environment

Previously, we found that *eg1* displayed a floral identity variation possibly influenced by growth conditions [53]. To examine if this variability was mainly due to the environmental alterations, we analyzed the spikelet phenotypes of *eg1-1* (in *indica* ZF802 background) and *eg1-2* (in *japonica* ZH11 background) in two groups of separate environments (Fig 1) and found that the floral phenotypic variability of *eg1* is likely caused by both genotype and environment. To define the phenotypic variability, we divided the spikelet phenotypes of *eg1* into six groups, which were called variable phenotypes, including W1 (WT-like), eg (extra glume), pl (palea to lemma), sp (smaller pa), le (long empty glumes) and rs (reiterated spikelets) (Fig 1A, S1 Fig and S1 Table). The results showed that sp and rs of *eg1-1* as well as W1, le, eg and sp of *eg1-2* exhibited significant plasticity between two environments, especially le of *eg1-2*, which displayed the highest plasticity (Fig 1B and 1C), suggesting that environment also contributes to the variations of floral phenotypes of *eg1*. To further examine the relationships of genotype (G), environment (E), genotype-environment interaction (GxE) and the variable phenotypes, we calculated their effects on phenotypes by two-factor ANOVA and found that W1 and pl were affected mainly by G, eg by both E and G but rarely by GxE, sp, le and rs by all three factors, and among them, le could serve as a marker for the phenotypic plasticity of *eg1-2* due to its large proportion in a panicle and opposite phenotypes between two environments (Fig 1A). Taken together, these results showed that *eg1* shows higher floral plasticity, suggesting that *EG1* promotes the floral robustness in rice.

Allelic *eg1* and their genetic backgrounds together regulate the *eg1* floral plasticity

To further examine the influence of genotype on the floral plasticity of *eg1*, we swapped the genetic backgrounds of two *eg1* alleles. *eg1-1* in a largely *japonica* background showed high

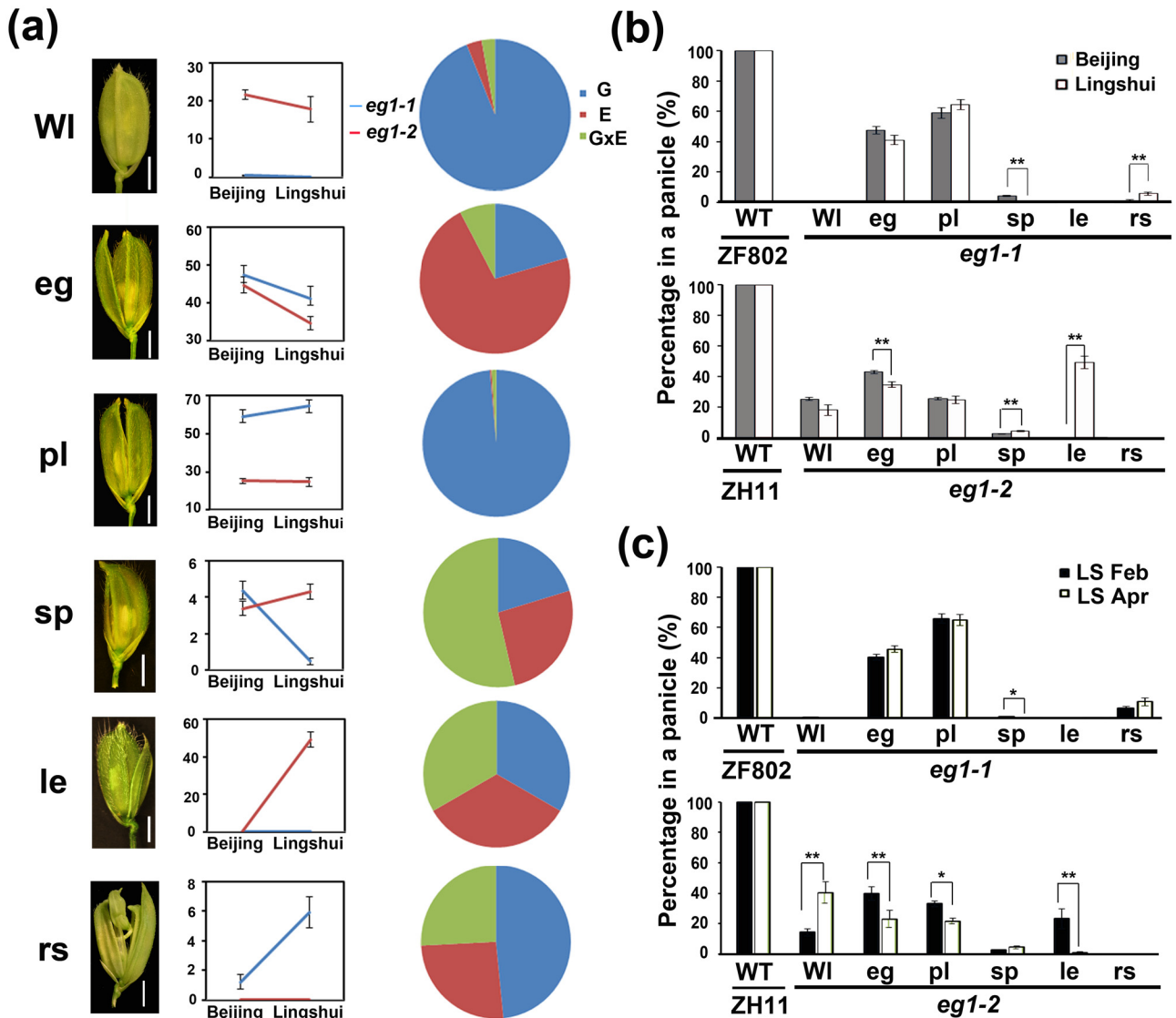


Fig 1. Phenotypic plasticity of floral identities of *eg1*. (a) Morphology and plasticity analysis of six variable phenotypes of *eg1* spikelets. Floral structures and two-factor plots with percentages per panicle in the y axis of all variable phenotypes are shown in the left and middle columns, respectively. Effects of G, E and GxE on each variable phenotype shown in the pie charts (right column) were analyzed by two-way ANOVA. Bar = 2 mm in floral structures. (b) Statistical analysis of the phenotypic plasticity of *eg1* and wild-type spikelets in two different planting locations. Beijing, Beijing summer. Lingshui, Lingshui winter. (c) Statistical analysis of the phenotypic plasticity of *eg1* and wild-type spikelet in two different planting seasons. LS Feb, Lingshui Feb. LS Apr, Lingshui Apr. WI, WT-like; eg, extra glume; pl, palea to lemma; sp, smaller pa; le, long empty glumes; rs, reiterated spikelets. Values are means \pm SE, number of analyzed panicles ≥ 20 in (b), ≥ 10 in (c). Significant difference was determined by ANOVA, *P < 0.05, **P < 0.01.

doi:10.1371/journal.pgen.1006152.g001

phenotypic plasticity especially for le and rs phenotypes, similar to *eg1-2* (ZH11), whereas *eg1-2* in an *indica*-dominant background showed low floral plasticity similar to *eg1-1* (ZF802) (Fig 2A), indicating that genetic backgrounds also influence the phenotypic plasticity of *eg1* spikelets.

To verify this finding, we further used CRISPR/Cas9 technology to construct *eg1* alleles in Nipponbare (*japonica*) and Dular (*indica*) backgrounds. Two types of spikelet phenotypes were found in *eg1-4* allele with Dular background and both showed low plasticity (Fig 2B), while *eg1-5* and -6 alleles in Nipponbare background showed relatively higher plasticity than

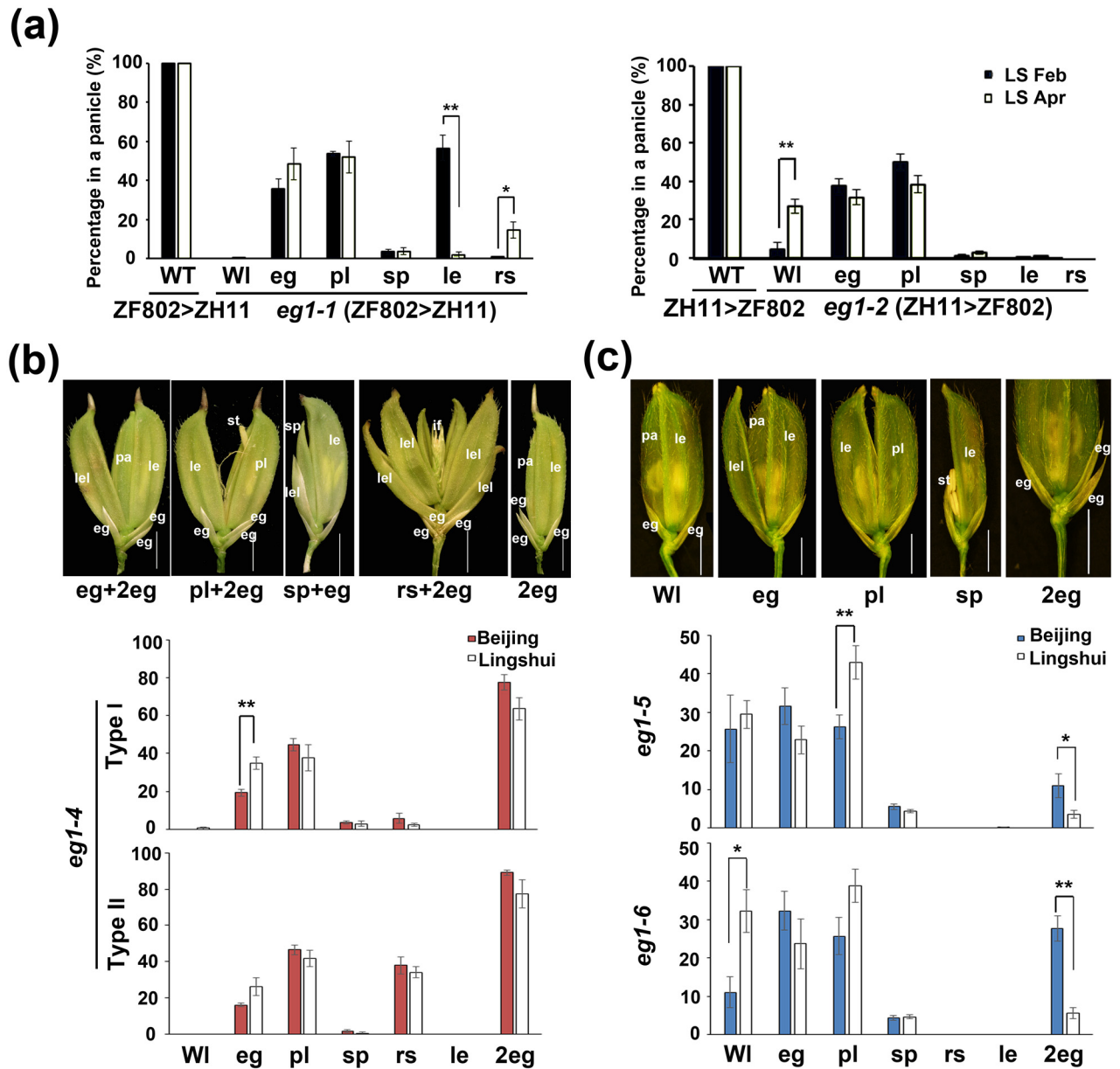


Fig 2. Subspecific variations of eg1 floral plasticity. (a) Floral plasticity of eg1 alleles in two exchanged backgrounds. eg1-1 and eg1-2 backcrossed into ZH11 or ZF802 backgrounds, respectively. (b) Floral plasticity of eg1-4 in *indica* Dular background. Statistical analysis of two types of panicles according to rs (Type I and Type II) are shown. (c) Floral plasticity of eg1-5 and -6 in *japonica* Nipponbare background. Statistical analysis of the two independent lines are shown. LS Feb, Lingshui Feb. LS Apr, Lingshui Apr. Beijing, Beijing summer. Lingshui, Lingshui winter. Variable phenotypes of spikelets are defined as in [S1 Table](#), and percentages of them in a panicle are shown in the y axis. le, lemma; pa, palea; st, stamen; eg, empty glume; if, inflorescence primordia; sp, smaller pa; lel, lemma-like organ; pl, palea-lemma mosaic organ. Bars = 2 mm. Values are means \pm SE, number of analyzed panicles ≥ 5 , and significant difference was determined by ANOVA, *P < 0.05, **P < 0.01.

doi:10.1371/journal.pgen.1006152.g002

alleles in two *indica* backgrounds ZF802 and Dular, similar to that in *japonica* ZH11 ([Fig 2C](#) and [S2 Fig](#)), suggesting that the floral plasticity of eg1 alleles in *japonica* backgrounds tend to be higher than that in *indica* backgrounds. In another aspect, eg1 alleles in *indica* backgrounds had severer floral disturbance than that in *japonica* concerning WI and rs phenotypes ([Fig 2](#) and [S1 Fig](#)), suggesting that EG1 has functions in both floral robustness and identity, which are

differentiated in two subspecies. To explore the possible causes of these differentiation, we compared the *cis*-elements and expressional level of *EG1* in several *japonica* and *indica* varieties and discovered the correlative differences in both *cis*-elements and expressional levels between *japonica* and *indica* (two types) varieties ([S3 Fig](#) and [S2 Table](#)), which implied that transcriptional differences may be a crucial cause of functional differentiation of *EG1* in subspecies. All these results indicated that both *eg1* allelic variations and their genetic backgrounds regulate the floral plasticity of *eg1*.

Temperature is a major environmental factor mediating the plastic development of *eg1* spikelets

In order to find out the environmental factors mediating the plastic development of *eg1* spikelets, we first compared the growing conditions for phenotypic analysis and found a marked difference in daily high temperatures of two environments ([S4 Fig](#)), suggesting that the temperature variation between two environments could be a major environmental factor influencing the *eg1* plasticity. To verify this prediction, floral plasticity of wild-types and *eg1* alleles were examined in two artificial growth chambers with 35°C light 12 hr / 20°C dark 12 hr and 25°C light 12 hr / 20°C dark 12 hr respectively, while other growth conditions were kept identical. The low plasticity of *eg1-1* and nearly 70% le phenotypes of *eg1-2* showed that the floral plasticity of *eg1* in the chambers was similar to and even higher than that under natural growth conditions ([Fig 3](#)). These results showed that temperature is a major environmental factor mediating the floral plasticity of *eg1*.

EG1 encodes a predominately mitochondria-localized functional lipase

Previously, *EG1* was shown to be localized in chloroplasts in transient expression assays [[54](#)]. However, *EG1*-like lipases appear to have variable subcellular locations [[56–59](#)]. To examine the subcellular localization of *EG1* *in vivo*, two different *EG1* and GFP fusion proteins driven by 35S promoter were first expressed in rice protoplasts and were found to be co-localized with both mitochondrial specific dye Mito Tracker Red and mitochondrial marker protein MTS-mOrange [[60](#)] but hardly with chloroplast auto-fluorescence, and an *EG1*-GFP fusion protein driven by native promoter was also detected in mitochondria ([Fig 4A and 4B](#)), suggesting that *EG1* protein is mainly, if not all, localized in mitochondria. To compare this finding with the previous one, the reported vector *pCAMBIA1301-Pro35S:EG1-GFP* [[54](#)] was also examined in our transient system and a similar localization was detected ([S5 Fig](#)). To further verify the *EG1* localization, subcellular fractionations of one-week seedlings of *eg1-2* complementation lines with FLAG-*EG1* ([S6 Fig](#)) were successively carried out and the *EG1* fusion protein was predominately co-fractionated with mitochondria ([Fig 4D](#)), confirming the mitochondrial localization of *EG1* *in vivo*. Taken together, these results showed that *EG1* encodes a protein predominately localized in mitochondria. To explore the biochemical function of *EG1*, we tested its lipase activity [[53](#)] *in vitro* and found that both the full-length *EG1* and truncated *EG1* without predicted targeting peptides showed significant lipase activity ([Fig 4E](#)), indicating that *EG1* encodes a functional lipase. Taken together, our results showed that *EG1* functions as a predominately mitochondria-localized lipase.

EG1 functions in a high temperature-dependent manner in the floral robustness regulation

The dependence of the *eg1* floral plasticity on environmental temperature raised a possibility that either *EG1* or its product or both are likewise regulated by temperature. To examine these

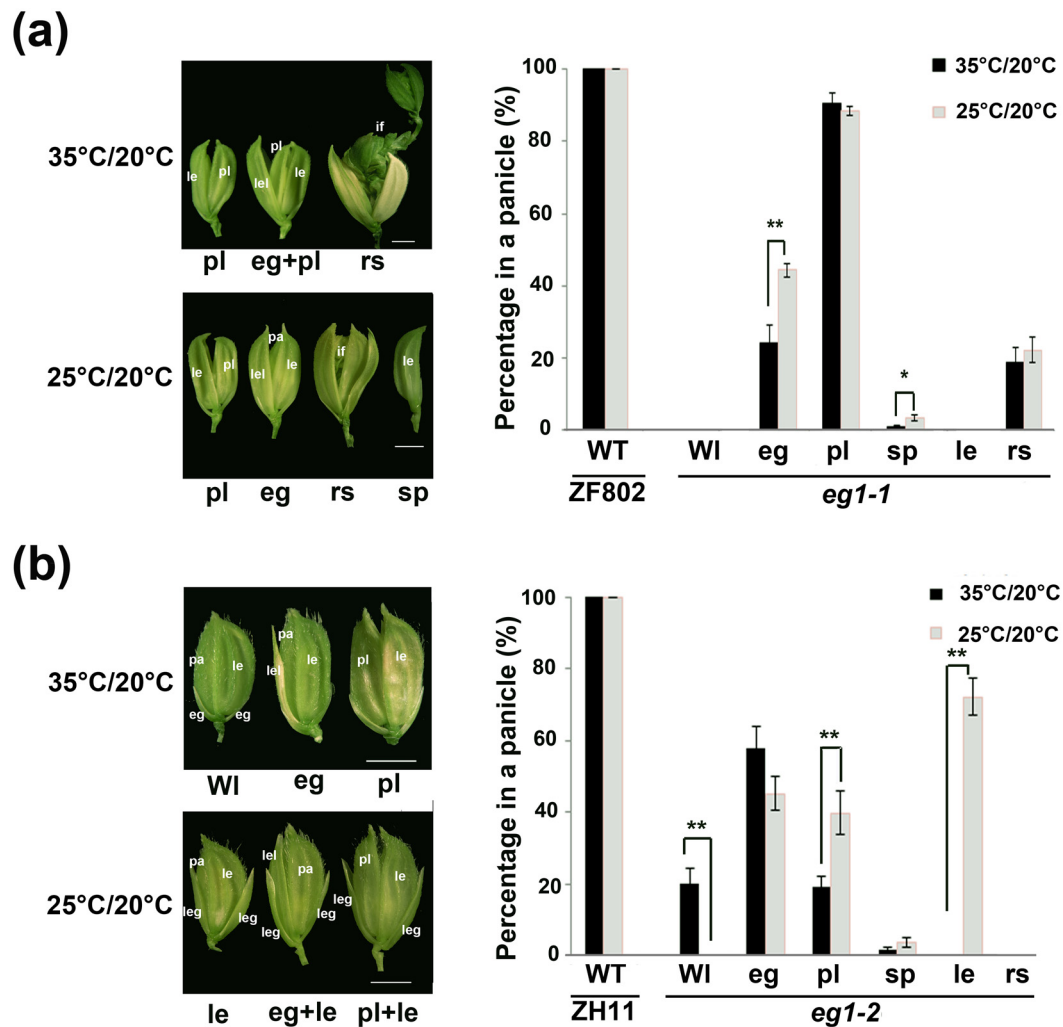


Fig 3. Temperature-dependent floral plasticity of *eg1*. (a) Floral plasticity of *eg1-1* (ZF802) under two different temperature conditions. (b) Floral plasticity of *eg1-2* (ZH11) under two different temperature conditions. Spikelet phenotypes and statistical analysis are shown in the left and right of (a) and (b). Variable phenotypes of spikelets are defined as in [S1 Table](#). le, lemma; pa, palea; eg, empty glume; if, inflorescence primordia; lel, lemma-like organ; pl, palea-lemma mosaic organ; leg, long empty glume in spikelet structures. Bars = 2 mm. Values are means ± SE, number of analyzed panicles >10, and significant difference was determined by ANOVA, *P < 0.05, **P < 0.01.

doi:10.1371/journal.pgen.1006152.g003

possibilities, some heat/cold responsive cis-elements were discovered in the 2 kb genomic sequence upstream of the start codon of *EG1* ([S3 Table](#)), implying that its expression could be induced by extreme temperatures. To examine this possibility, one-week wild-type seedlings were treated under different temperatures and the *EG1* transcript was found to accumulate gradually, to an extremely high extent under heat shock (42°C) as well as usual high temperature 35°C for rice ([Fig 5A](#)), but to some extent suppressed under cold stress (4°C) ([S7A Fig](#)), indicating the high temperature-induced expression of *EG1*. A similar result was obtained by using young inflorescences in which *EG1* has a high expression ([S7B Fig](#)). To examine whether *EG1* protein was also influenced by high temperatures, accumulation of FLAG-*EG1* fusion protein in *eg1-2* complementation lines, with a temperature-insensitive promoter ([S7C and S7E Fig](#)), was detected under different temperatures and found it was significantly induced at

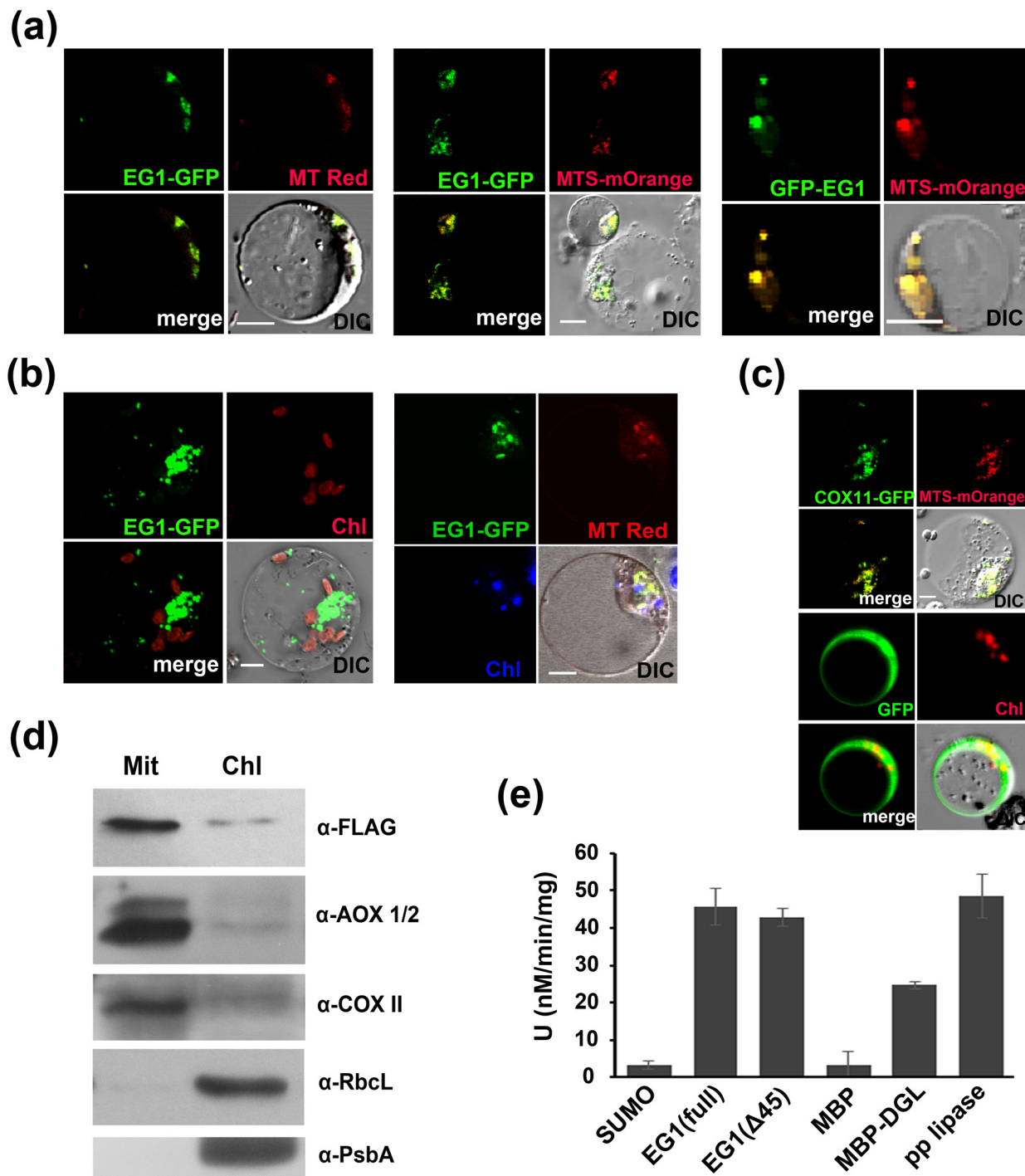


Fig 4. EG1 encodes a functional lipase predominately localized in mitochondria. (a) Co-localization of EG1-GFP or GFP-EG1 fusion protein with mitochondria in rice protoplasts. Mitochondria are marked by dye Mito Tracker Red (MT Red) or MTS-mOrange protein. (b) Localization analysis of EG1-GFP and chloroplasts in rice protoplasts. An EG1-GFP driven by 35S or native promoter is shown in the left and right, respectively. Chloroplasts are detected by its auto-fluorescence. Mitochondria are marked by Mito Tracker Red (MT Red). (c) Localization of mitochondrial (35SPro:COX11-GFP) [60] (up) and cellular (35SPro:GFP) (bottom) controls of rice protoplasts. DIC, pictures photographed by differential interference contrast microscope. Bar = 10 μm. (d) Subcellular fractionation assay. Mit, mitochondria fraction; Chl, chloroplasts fraction; α-FLAG, antibody of FLAG-EG1; α-AOX1/2 and α-COXII, specific antibodies of mitochondrial proteins AOX1/2 and COXII; α-RbcL and α-PsbA, specific antibodies of chloroplast proteins RbcL and PsbA. (e) Lipase activity of EG1 in vitro with P-nPB as a substrate at 30°C. EG1 (Full) and EG1 (Δ45) respectively refer to fusion proteins of full-length or no N-terminal (45 aa) protein of EG1 and SUMO peptide. DGL and pp lipase (porcine pancreatic lipase) were used as positive controls. Values are means ± SE for three independent experiments.

doi:10.1371/journal.pgen.1006152.g004

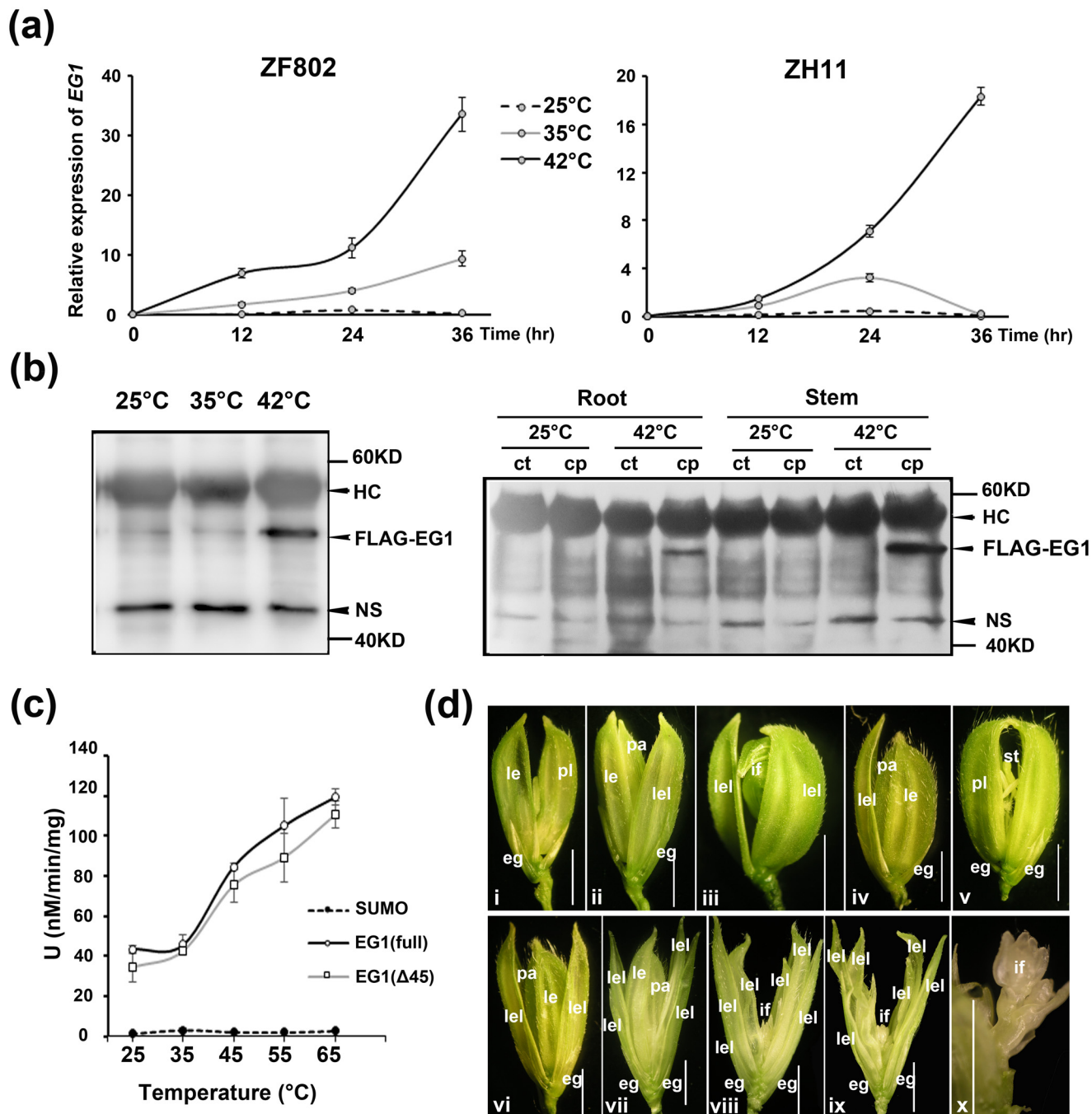


Fig 5. High temperature-dependent manner of EG1 in floral robustness regulation. (a) RT-qPCR analysis of EG1 expression induced by high temperatures in two wild-types. Values are means \pm SE ($n = 3$), and significant difference was determined by ANOVA, *P < 0.05, **P < 0.01, and rice α -TUBULIN as the reference. (b) Western blot analysis of FLAG-EG1 protein accumulation under different temperatures and different tissues in the EG1 complementation lines for 24 hr. Cp, Complementation lines; Ct, non-transgenic wild-type control. HC, Heavy chain of IgG; NS, Nonspecific band (as a loading control). (c) Temperature-dependent lipase activity of EG1. EG1 (Full) and EG1 (Δ 45) respectively refer to full-length and no N-terminal (45 AA) protein of EG1 fused to SUMO peptide. Values are means \pm SE for three independent experiments. (d) Floral phenotypes of eg1 mutants in a condition of 40°C light 12 hr / 30°C dark 12 hr. Spikelets of eg1-1 with pl, eg and rs phenotypes are shown on i, ii and iii, respectively. Spikelets of eg1-2 with eg and pl phenotypes are shown on iv and v, and with multilayer lemma-like glumes (lel) and/or undetermined inflorescence primordia are on vi to x. x is the inside of ix. le, lemma; pl, palea-lemma mosaic organ; eg, empty glume; lel, lemma-like organ; pa, palea; st, stamen; if, inflorescence primordia. Bars = 2 mm.

doi:10.1371/journal.pgen.1006152.g005

extreme high temperature 42°C than 25°C and 35°C ([Fig 5B](#) and [S7D Fig](#)), indicating a stabilization of EG1 protein under heat stress. Furthermore, we detected that lipase activity of EG1 fusion proteins increase as temperature rising ([Fig 5C](#)), consistent with the assumption of EG1's function required under high temperatures. Additionally, we also examined the effect of high temperatures on EG1 subcellular localization, and found no obvious translocation in protoplast system ([S8A Fig](#)), while failed to detect EG1 protein in the subcellular fractions of complementation lines except under heat stress for its minute amount ([S8B Fig](#)), suggesting that temperature does not significantly influence the subcellular localization of EG1. The increased transcriptional level, protein stability and lipase activity of *EG1* under high temperatures, implying its more significant role under high temperatures. To verify this hypothesis, we observed the floral phenotypes of *eg1* mutants under extremely high temperatures and found much severer spikelets in *eg1* mutants especially in *eg1-2*, with multilayer lemma-like organs and undetermined inflorescence meristem, which have never been found in other temperature conditions ([Fig 5D](#)), showing a more significant function of *EG1* at higher temperatures in floral robustness. *eg1* was also found to grow faster than wild-type during primary growing days [54], and we detected this phenotype was much severer under extremely high temperature than others compared with wild-type, which was consistent with the floral phenotype ([S9 Fig](#)). Therefore, we concluded that *EG1* functions in a high temperature-dependent manner to regulate the floral robustness.

EG1 mediates the transcriptional responses of downstream genes and pathways to environmental fluctuation

Since the floral plasticity of *eg1* was influenced by both genotype and environment, to examine the molecular mechanism of genotype-environment interaction in floral plasticity, transcriptomes of inflorescences of two *eg1* alleles (*eg1-1* and *eg1-2*) and their wild-types (ZF802 and ZH11) in Beijing and Lingshui were analyzed. First, to evaluate the reliability of the transcriptomic data, we divided all transcripts into 33 modules by co-expression network analysis and analyzed their correlations with six variable phenotypes, and it turned out that the relationships among the variable phenotypes derived from these correlations were quite similar to their morphological correlations ([S10 Fig](#)), showing a good reliability of the transcriptomic data. Second, through overall comparisons of all transcriptomes, we discovered that the expression patterns of floral transcriptomes of *eg1* alleles between two environments were significantly different from their wild-types ([S11A Fig](#)), indicating a role of *EG1* in regulating expressions of environmentally responsive genes. The numbers of environmentally responsive genes in *eg1* mutants were much larger than that of wild-types, in contrast to the similar numbers between two wild-types or two *eg1* alleles ([Fig 6A](#) and [S11B Fig](#)), implying that *EG1* negatively regulates the responses of its downstream genes to environment. To verify this finding, we analyzed the effects of G, E, and GxE on transcriptomes of *eg1* and wild-type by two-way ANOVA and found that the number of genes significantly affected by E and GxE in *eg1* were significantly larger than that in wild-types ([Fig 6B](#), [S11C Fig](#) and [S4 Table](#)), displaying a switch of many genes from G-affected to E/GxE-affected ones ([Fig 6C](#)), indicating that *EG1* represses its downstream genes not only to respond to, but also to interact with environment. Furthermore, the effects of the three factors on several important pathways varied significantly between *eg1* and wild-type, including the pathways related to temperature response, lipid metabolism and floral development ([Fig 6D](#) and [S5 Table](#)), indicating that *EG1* mediates a crosstalk of these pathways with environment. Since *EG1* was reported to regulate JA biosynthesis [54], in order to analyze its effect on the floral robustness control, we examined the expressional patterns of JA biosynthesis and signaling associated genes in our transcriptome

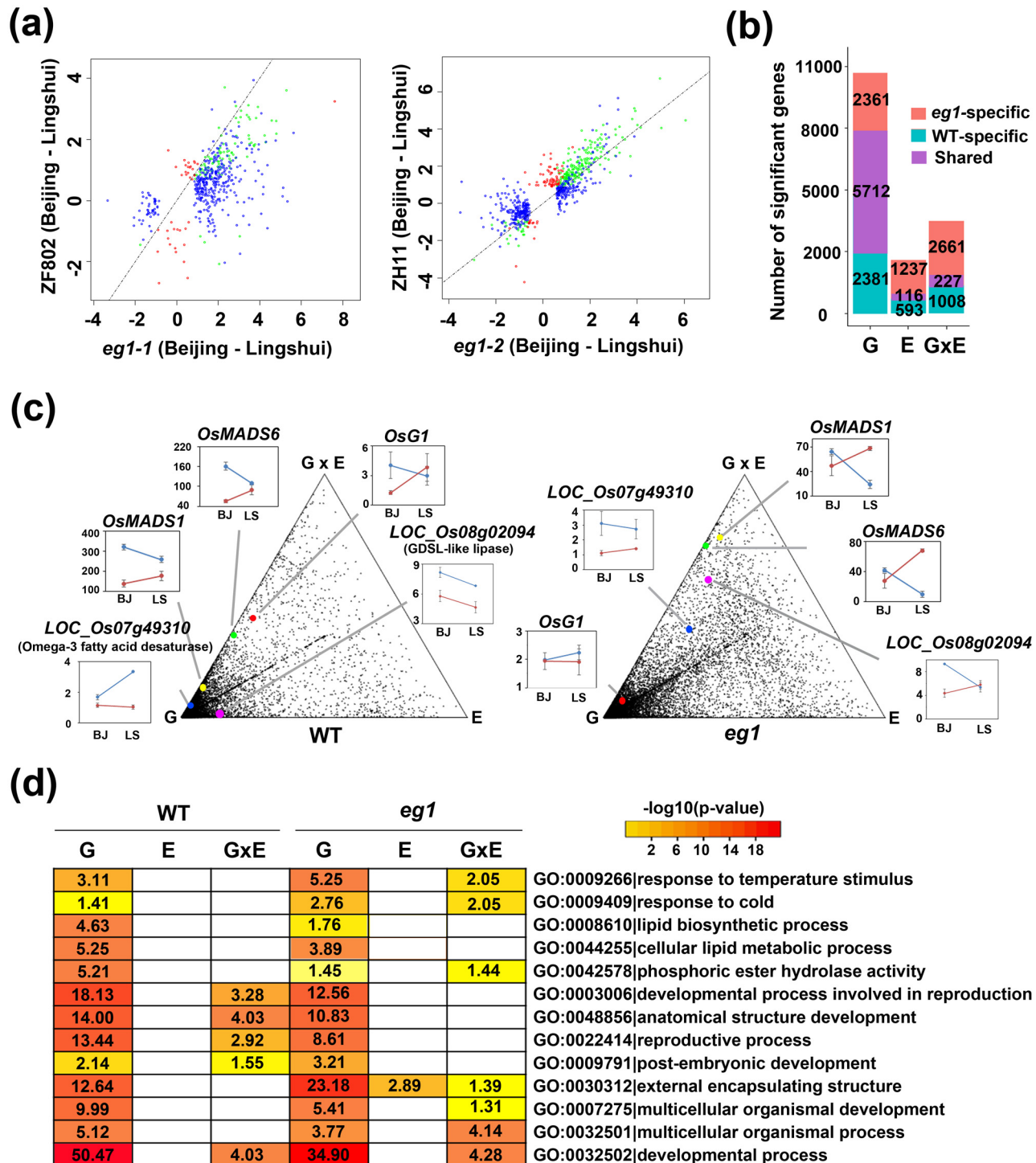


Fig 6. Genotype (G), environment (E) and genotype-environment interaction (GxE)-dependent gene expressional variations of *eg1*. (a) Scatterplots of comparisons of environmentally responsive genes between *eg1* alleles and wild-types. x and y axes are values of \log_2 [ratios of gene expression in Beijing to that in Lingshui] of two genotypes respectively. Points represent wild-type-specific (red), *eg1*-specific (blue) and shared (green) genes. Dotted lines indicate $y = x$ lines. (b) Comparisons of genes significantly affected by G, E and GxE in wild-type and *eg1*. Effects were analyzed by two-way ANOVA. (c) Triangular scatterplots of distributions of genes significantly affected by G, E and GxE in wild-type and *eg1*. Each dot indicates a gene, and the three vertexes of triangle indicate three factors G, E, GxE respectively. The closer distance between a gene and a vertex means the stronger effect of the factor on the gene. Insets show expressions of some representative genes in ZF802/*eg1*-1 (blue lines) and ZH11/*eg1*-2 (red lines) of Beijing (BJ) and Lingshui (LS). Effects were analyzed by two-way ANOVA. (d) Comparisons of thirteen major pathways affected by G, E and GxE in wild-type and *eg1*. Numbers

in boxes indicate -log₁₀ (P-value) of the pathway enrichment tested by Fisher's exact test with Bonferroni correction and blank boxes no statistical significance.

doi:10.1371/journal.pgen.1006152.g006

data, and found that the transcriptional responsive patterns to environment or transcriptional level of several JA signaling genes (*JAZ7* and *JAZ8*) and JA biosynthesis genes (four methyltransferase genes) are varied in *eg1* mutants ([S12 Fig](#)), implying a possible role of JA in the *EG1*-associated floral robustness regulation but different from previously reported [[54](#)]. Taken together, these results revealed that *EG1* mediates the transcriptional responses of downstream genes and pathways to environmental fluctuation.

OsMADS1, OsMADS6 and OsG1 act downstream of EG1 to mediate floral robustness regulation

The significant transcriptional effects on the floral development pathways based on the G, E and GxE analysis in *eg1* mutant suggested that floral identity genes are likely involved in *EG1*-dependent floral robustness regulation. To examine this, expressional variation of thirteen floral identity genes between two environments were further analyzed, and seven (OsMADS1, OsMADS6, OsG1, OsMADS4, OsMADS7, OsMADS8, OsMADS58) of them showed both varied environment-dependent expression patterns and repressed expression levels in *eg1* ([S13 Fig](#)), indicating their positive regulatory roles in the floral robustness. To further examine this possibility, genetic analysis between *EG1* and three of them (OsMADS1, OsMADS6 and OsG1) were performed. OsMADS1 and OsMADS6 are two major genes regulating glume identity and floral determinacy in rice [[61–69](#)], and their expressions were significantly varied in *eg1* ([Fig 7E](#) and [S13 Fig](#)), indicating that *EG1* is required for their expressions. To examine their genetic relationships with *EG1*, a double mutant of OsMADS1 mutant allele *nsr* [[61](#)] and *eg1-1* was generated and it exhibited longer and leafy lemmas/paleas similar to *nsr*, with all inner three whorls replaced by half-developed inflorescences or inflorescence primordia, which is severer than both single mutants ([Fig 7B](#)), indicating that OsMADS1 functions downstream of *EG1* in lemma/palea identity and they may together regulate the determinacy of inner three whorls. In addition, the double mutant of *eg1-1* and OsMADS6 mutant allele *osmads6-5* [[66](#)] showed abnormal paleas, with all transformed into one or two small lemma-like glumes and mostly with inflorescence primordia inside the spikelets ([Fig 7C](#)), indicating that OsMADS6 functions downstream of *EG1* in specifying palea but may also regulate floral determinacy together with *EG1*. *osmads6-5* exhibited weaker floral disturbance in the F2 population when crossed with *eg1-1* (ZF802), with lemma-palea mosaic paleas and usually normal inner whorls ([Fig 7C](#)), showing its floral phenotype is also greatly influenced by genetic backgrounds. To further examine the relationships among *EG1*, OsMADS1 and OsMADS6 especially in floral determinacy, *nsr osmads6-5* and *eg1-1 nsr osmads6-5* were successively generated. The floral meristems of these two mutants similarly generated continuous glume primordia or became inactive before inner three whorls developed ([Fig 7D](#)), which were more dedifferentiated than the inflorescence primordia of *eg1-1 nsr* and *eg1-1 osmads6-5*, supporting the findings that both OsMADS1 and OsMADS6 act downstream of *EG1* and they together control the floral differentiation of inner three whorls. Compared with *eg1-1*, the rs plasticity of *eg1-1 nsr osmads6-5* totally disappeared when these two MADS genes were both deficient ([Fig 7B and 7D](#)), supporting the important roles of OsMADS1 and OsMADS6 in the rs plasticity regulation. Additionally, the spikelet phenotype of *eg1-1 nsr* [[54](#)] and *nsr osmads6-5* [[68,69](#)] were consistent to the previously reported, and *eg1* was linked with the lemma-like (lel) structure, and not affected by the deficiency of OsMADS1 and OsMADS6 ([Fig 7b–7d](#)), implying that it is probably a special

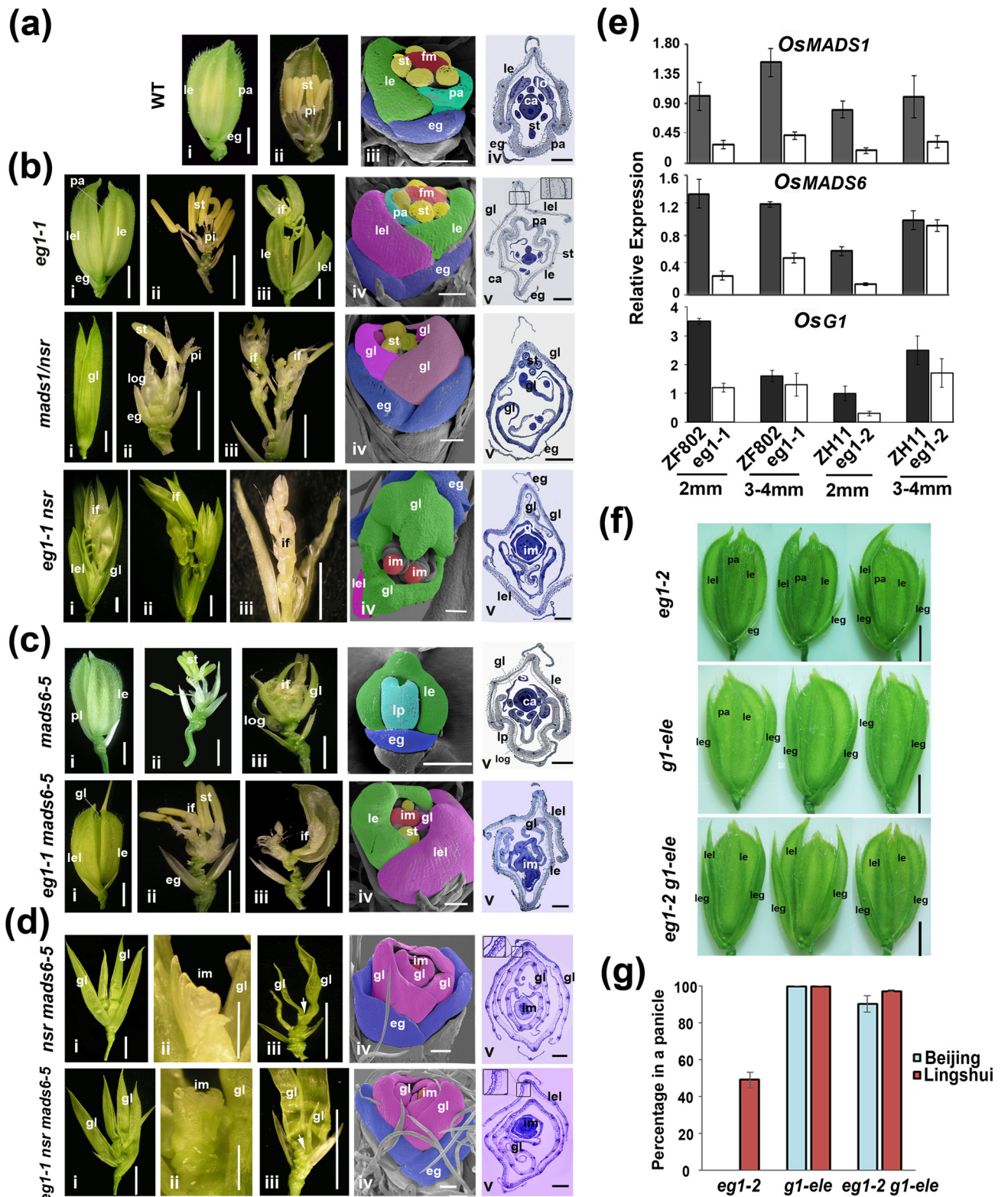


Fig 7. *OsMADS1*, *OsMADS6* and *OsG1* mediate the floral robustness regulation of *EG1*. (a) Spikelets of wild-type rice. i-iv show outside (i), inside (ii), SEM (iii) and paraffin transverse section (iv) of wild-type spikelets, respectively. (b) Genetic analysis of *eg1-1* and *mads1/nsr*. Photos show the outside (i), inside (ii-iii), SEM (iv) and paraffin transverse section (v) of *eg1-1*, *mads1/nsr* and *eg1-1 nsr* mutant spikelets, respectively. (c) Genetic analysis of *eg1-1* and *mads6-5*. Photos of *mads6-5* and *eg1-1 mads6-5* are shown as (b). (d) Genetic analysis of *nsr mads6-5* and *eg1-1 nsr mads6-5*. Photos show the outside (i), inside (ii-iii), SEM (iv) and paraffin transverse section (v) of *nsr mads6-5* and *eg1-1 nsr mads6-5* mutant spikelets, respectively. (e) Relative Expression of *OsMADS1*, *OsMADS6* and *OsG1* across genotypes. ZF802 is used as a reference. Error bars represent standard deviation. (f) Photos of *eg1-2*, *g1-ele*, *eg1-2 g1-ele* genotypes in a panicle. (g) Percentage of *eg1-2* and *g1-ele* genotypes in a panicle for Beijing and Lingshuai varieties.

eg1-1 and *nsr mads6-5*. Photos of *nsr mads6-5* and *eg1-1 nsr mads6-5* are shown as (b). Arrows on iii of *nsr mads6-5* and *eg1-1 nsr mads6-5* indicate the inactive growing points. (e) Relative expression levels of *OsMADS1*, *OsMADS6* and *OsG1* in wild-type and *eg1* inflorescences of different growth stages by RT-qPCR. Results are means ± SE. Rice α -TUBULIN was used as the reference. (f) Genetic analysis of *eg1* and *g1-ele*. Empty glume phenotypes of *eg1-2* in Lingshui, *g1-ele* and *eg1-2 g1-ele* in Beijing/Lingshui are shown respectively. (g) The phenotypic plasticity of le in *eg1-2*, *g1-ele* and *eg1-2 g1-ele*. Values are means ± SE, number of analyzed panicles ≥ 5. le, lemma; pa, palea; st, stamen; pi, pistil; eg, empty glume; ca, carpel; fm, floral meristem; im, inflorescence meristem; if, inflorescence primordia; lel, lemma-like organ; gl, glume-like organ; lp, lemma-palea mosaic organ; log, lodicule-glume mosaic organ. leg, long empty glume. Bars = 2 mm, 200 μ m and 200 μ m in spikelet structures, SEMs and paraffin transverse sections respectively, except for 0.5 mm in ii of (d).

doi:10.1371/journal.pgen.1006152.g007

organ different from lemma and palea. Taken all these results together, we concluded that *MADS1* and *MADS6* together function downstream of *EG1* to control the determinacy of inner three whorls of rice floret as well as to mediate the rs plasticity of *eg1-1*.

Furthermore, the le phenotype (long empty glume) of *eg1-2* has the highest plasticity among all variable phenotypes (see Figs 1–3), and *OsG1* (*Long Sterile Lemma*) and *OsMADS19/34* are two crucial genes suppressing the elongation of empty glumes in rice [70–72]. The expression levels and patterns of *OsG1* but not *OsMADS19/34* appeared to be aberrant in *eg1-2* (Fig 7E and S13 Fig), implying that *OsG1* may contribute to the le phenotype of *eg1-2*. To confirm this, *g1-ele* allele of *OsG1* [72] was used to obtain a double mutant by crossing with *eg1-2*, and it turned out that almost all empty glumes of *eg1-2 g1-ele* were elongated to lemma-like organs similar to *g1-ele*, exhibiting much lower plasticity compared with *eg1-2* (Fig 7F and 7G), indicating that *OsG1* functions downstream of *EG1* in regulating empty glume development and contributes to the plastic le phenotype of *eg1-2*. Taken together, these results show that *OsMADS1*, *OsMADS6* and *OsG1* all act downstream of *EG1* to mediate the floral robustness regulation.

Discussion

EG1 is a plasticity gene regulating the floral robustness against environmental fluctuation in rice

To our knowledge, no plasticity genes have been confirmed to function in floral robustness in flowering plants [47–52]. Given the sessile nature of plant species, uncovering this class of genes and dissecting their molecular mechanisms are crucial for understanding the biology of flower development and evolution. In this study, we have shown that *EG1* encodes a mitochondria-localized lipase functioning as a plasticity gene to regulate the rice floral robustness by a coordinated transcriptional regulation of temperature, lipid metabolism and flower development pathways. First, *eg1* alleles showed floral variations under both natural and artificial conditions and five *eg1* alleles produced increased floral plasticity. Second, RNA expression, protein stability and lipase activity of *EG1* can respond to environment enhancing its function significantly in severe conditions such as heat stress. Third, *EG1* appears to possess a “buffering” function of repressing environmental stimuli to interfere the target genes, and when environmental pressure becomes severer such as heat stress, the strengthened *EG1* function induced by heat is enough to buffer the stronger and more deleterious effect of heat on the responsive transcriptional pathways. Last, *EG1* influences the expression of numerous floral identity genes, which are the direct contributors of plastic development of *eg1* spikelets. Thus, *EG1* is the first plasticity gene regulating plant floral robustness against environmental fluctuation. Our finding indicates that flowers retain a system containing *EG1* to sense and respond to environmental stimuli to maintain its stable development, and suggests a mechanism of transition from high plasticity to robustness in flower by recruiting plasticity-repressing genes, which ensures the coordinated development of organs with different plasticity in one organism.

Mitochondria could serve as a hub for the lipid metabolism mediated-floral developmental robustness

Lipid metabolisms are known to be involved in adaptive plasticity of organisms [36,37,41,42], and mitochondria, as the energy factory of eukaryotes and one of subcellular compartmentations of lipid metabolism, have been reported to be crucial to the adaptive stability of plant vegetative traits [41,43,44]. As EG1 is a predominately mitochondria-localized functional lipase, our results suggest that the mitochondria-mediated lipid metabolism plays an important role in the regulation of floral robustness against temperature fluctuation. However, it remains unclear how this could be carried out. It is likely that mitochondria-related lipid homeostasis could serve as a “buffer” to relieve the effect of environmental stimuli and mediate the temperature-dependent floral plasticity regulation (Fig 8). Recently, *EG1* has been shown to influence JA synthesis, and JA signaling pathway regulates the transcription of floral identity gene *OsMADS1* [54], showing that JA potentially mediates the crosstalk of *EG1* and flower development related transcriptional factors. In fact, the most homologous gene of *EG1* in Arabidopsis *DGL* has been verified to function in JA biosynthesis [55,56,73], though its chloroplast location was questioned [55], suggesting that a non-chloroplast localized lipase is likely to function in JA production (Fig 8). On the other side, we may fail to detect *EG1* protein due to its minute amounts in chloroplasts. Furthermore, according to the much severer phenotype of *eg1* and *eg2-1D* (a mutant allele of *EG2/OsJAZ1*) double mutant compared with two single [54], we noticed that JA signaling may be not the only pathway activated by *EG1* to mediate the signal transduction from outside to inside of nucleus in the *EG1*-associated floral regulation, other lipid-related pathways and regulatory mechanisms are also possible (Fig 8).

Functional divergence of *EG1* and its homologs in angiosperms

In our study, *eg1* alleles showed a higher floral plasticity in *japonica* than that in *indica* varieties, while a severer floral disturbance in *indica*, revealing a functional divergence of *EG1* in rice subspecies. No differences in coding sequences but *cis*-elements of *EG1* in two subspecies were detected (S14 Fig), implying that this subspecific variation might be caused by an unknown differential responsive capability of promoters to environmental or endogenous stimuli. Besides, since genetic backgrounds are known to influence developmental outcomes via phenotypic modifiers [74,75], there also may be some *indica-/japonica*-specific modifiers to modulate *EG1* function due to their different genetic backgrounds, which can be either epistatic genes or specific lipid substrates of *EG1* required for floral developmental robustness. Genetic dissection of these subspecific modifiers of plasticity will provide further insights into the molecular mechanism of floral development. So far, all reported *EG1* homologs in dicots have no apparent plasticity function in flowers [56–59], and *EG1* homologs in monocots can be mainly divided into two clades, one similar to that in dicots and the other unique to monocot species based on the phylogenetic tree and predicted subcellular localizations (S13 Fig), we thus speculate that *EG1* may have acquired a monocot-specific neofunctionalization in promoting floral robustness. Detailed genetic and biochemical analyses of these genes would provide additional clues to when and how the plasticity function and the subspecific divergence of *EG1* arose in monocot species.

In conclusion, our results revealed a novel function of *EG1* in floral developmental robustness against environmental fluctuation by mediating the mitochondrial lipid metabolism. Our finding also provide a genetic means to maintain the stable flower development under environmental stress ensuring grain yield stability in rice and potentially in other monocot species. Further studies should unlock the molecular crosstalk between mitochondria and nucleus in regulating floral developmental robustness.

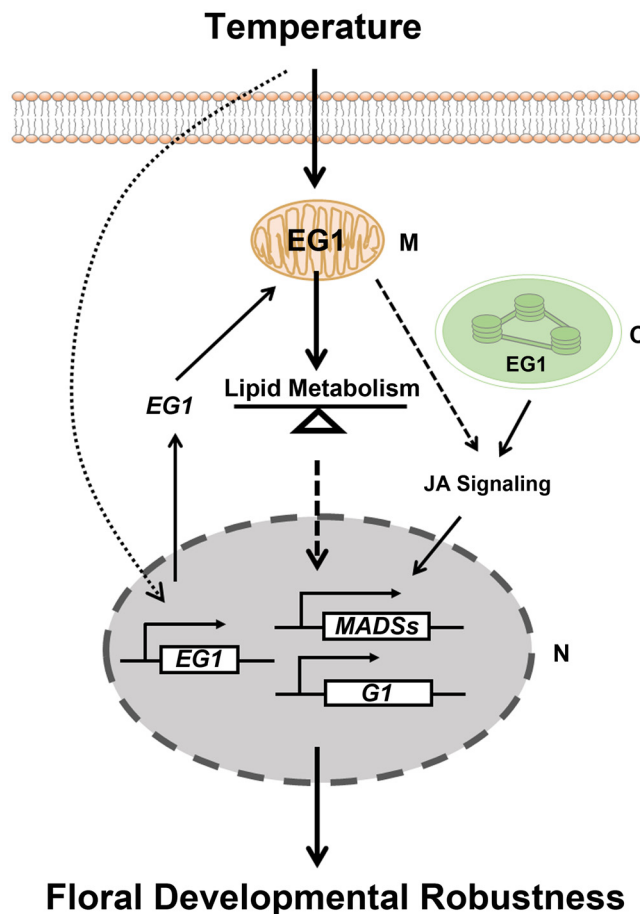


Fig 8. A model for *EG1* in regulating floral developmental robustness against temperature fluctuation in rice. *EG1* responds high temperature fluctuation at its transcriptional, posttranscriptional and lipase activity levels, and positively regulates the transcriptions of floral identity genes such as *OsMADS1*, *OsMADS6* and *OsG1*, which are mediated by a mitochondria-associated lipid metabolism, resulting in floral developmental robustness against temperature fluctuation. Additionally, chloroplasts-localized *EG1* has also been shown to regulate the transcription of floral identity gene *OsMADS1* through JA signaling pathway [54].

doi:10.1371/journal.pgen.1006152.g008

Materials and Methods

Plant materials, growth conditions and spikelet phenotypic analysis

Five rice *eg1* recessive alleles were used in this study. *eg1-1* and *eg1-2* were from our previous work [53], in backgrounds of *O. sativa* L. spp. *indica* Zhefu 802 (ZF802) and *O. sativa* L. spp. *japonica* Zhonghua 11 (ZH11) respectively. *eg1-4* was generated from *indica* Dular, and *eg1-5* and -6 from *japonica* Nipponbare by CRISPR/Cas9 technology [76,77]. Besides, ZF802>ZH11 and *eg1-1* (ZF802>ZH11) were isolated from an F2 population of ZF802 wild-type or *eg1-1* backcrossed with ZH11 three times, and ZH11>ZF802 and *eg1-2* (ZH11>ZF802) were isolated from an F2 population of ZH11 wild-type or *eg1-2* backcrossed with ZF802 once. Other rice mutants, *nsr* [61] and *g1-ele* [72] were kindly provided by Dr. Zhukuan Cheng, and *osmads6-5* also from our previous work [66].

Plants were grown in the natural conditions of Beijing (China) from Mar. to Oct. and Lingshui (Hainan province, China) from Dec. to Apr. (year 2014~2015). Weather data of 2014.7.28~2014.8.17 of Beijing and 2014.3.15~2014.4.4 of Lingshui, and 2014.2.1~2014.2.20 and 2014.4.1~2014.4.20 of Lingshui were shown respectively, which were ranged from ten days

before spikelet meristem formation (~2 mm) to ten days after that. Artificial conditions in chambers were 35°C light 12 hr / 20°C dark 12 hr, 25°C light 12 hr / 20°C dark 12 hr and 40°C light 12 hr / 30°C dark 12 hr, respectively, with identical light intensity 50 $\mu\text{mol m}^{-2} \text{s}^{-1}$ and relative air humidity 60%.

Spikelets of *eg1* were divided according to phenotypes of outer glumes (lemma, palea, empty glumes and extra glumes) following two rules: (1) the most significant mutant phenotype of *eg1* is in the outer glumes; (2) outer glumes have linkages with inner organs: normal palea always linked with normal inner organs, lemma-like palea with increased stamens and pistils, smaller palea with decreased stamens, multilayer glumes linked with rs. Main panicles/inflorescences of plants at booting stage were used for phenotypic analysis. Percentages of all variable phenotypes in one panicle were calculated for comparisons, and in some cases more than one phenotype appeared in a single spikelet. Data were statistically analyzed by using one/two-way ANOVA (Excel). Effects of genotype, environment and genotype-environment interaction on all variable phenotypes were calculated using phenotypic statistic data of *eg1* and wild-type grown in Beijing summer and Lingshui winter by two-way ANOVA. In CRISPR experiment, more than six independently homozygous lines were generated in each background, and their phenotypes were quite similar, thus only one/two lines were statistically analyzed and shown in our results.

Protein subcellular localization analyses

Full-length *EG1* CDS was inserted into N- or C-terminal of GFP sequence of vector *pBI221-35SPro:GFP*, and full-length *EG1* CDS with 1.5 kb native promoter into *pCAMBIA1301-GFP*. *MTS-mOrange* and *Pro35S:COX11-GFP* plasmids were kindly provided by Dr. Yaoguang Liu [60], and the reported vector *pCAMBIA1301-35SPro:EG1-GFP* was provided by Dr. Dabing Zhang [54]. All plasmids of high quality were prepared for protoplast transfection. Rice protoplast preparation from 2-week-seedlings grown in light and polyethylene glycol (PEG)-mediated transfections were performed as described by Bart et al. [78]. Images were captured by a confocal microscope (FluoView 1000, Olympus).

Floral disorder of *eg1-2* was complemented by genetic transformation using vector *pTCK303-ProUBIQUITIN:FLAG-EG1*. One-week seedlings of *EG1* complementation lines were used for subcellular fractionation. Fractionations of mitochondria and chloroplasts were performed as described by Rodiger et al. [79]. After precipitating the organelle fractions, western blots were performed with α -FLAG (Sigma), mitochondria specific antibodies α -AOX1/2 and α -COXII (Agrisera), and chloroplasts specific antibodies α -RbcL and α -PsbA (Agrisera). Fractionation assays were performed with two independent complementation lines.

Lipase activity analysis in vitro

Full-length *EG1* CDS and a truncated *EG1* CDS without predicted targeting sequence (135 bp) with engineered N-terminal SUMO tag were separately cloned into *pET-30a* (Novagen) to generate His6-SUMO-tagged fusion proteins. Mitochondrial targeting sequence was predicted with MitoProt II online [80]. *DGL* CDS without targeting sequence [81] was introduced into vector *PMAL-C2X* (NEB). All the fusion proteins were expressed in *E. coli* BL21 (DE3). The His₆-SUMO-tagged fusion proteins were purified using Ni-NTA (Novagen) and eluted with buffer containing 25 mM Tris-HCl (pH 7.4), 150 mM NaCl and 250 mM imidazole. The MBP-tagged fusion proteins were purified using amylose resin (NEB) and eluted with buffer containing 50 mM Tris-HCl (pH 7.4) and 10 mM amylose. Imidazole in protein solutions was removed with desalting columns (Thermo Scientific) before lipase activity analysis.

p-nPB (p-nitrophenyl butyrate, Sigma) was used as the substrate of lipase analysis in vitro. Colorimetric assays for lipase activity of fusion proteins were performed as described by Seo

et al. [82] with some modifications. A solution containing 1.11 mg/mL p-nPB (dissolved with isopropanol) and B solution containing 50 mM Tris-HCl (pH 7.4) and 0.1% Arabic gum were first prepared. Reactive solution was composed of 1 volume A solution and 9 volumes B solution with 2% Triton X-100. About 20 μ L purified proteins (~5 μ g) and 180 μ L reactive solution were used for each reaction. After incubated under different temperatures for 30 min, p-nitrophenol formation from p-nitrophenyl butyrate was determined spectrophotometrically at 405 nm by an ELISA microplate reader. DGL and porcine pancreatic lipase (Sigma) were used for positive controls, and p-nitrophenol (Sigma) for the standard curve.

Physiological experiments

Cis-elements in the genomic sequence upstream of the start codon of *EG1* was analyzed by PLACE online [83]. Wild-type ZF802, ZH11 and *EG1* complementation lines were grown at 25°C for one week after germination, and wild-type ZH11 seedlings were grown in a consistent condition till 2 mm inflorescence meristem developed before being treated under different temperatures for different time. The transcripts of *EG1* and *FLAG-EG1* were analyzed by RT-QPCR or RT-PCR. The root and shoot phenotypes of seedlings were statistically analyzed after growing under consistent temperatures for six days after germination. Other condition parameters of physiological experiments were daylight 12 hr, light intensity 50 μ mol m $^{-2}$ s $^{-1}$ and relative air humidity 60%. We use 42°C as an extremely high temperature for short treat but 40°C for long treat by considering the tolerance of plants.

FLAG-EG1 protein in *EG1* complementation lines was enriched by immunoprecipitation for its small amount and detected by western blot with α -FLAG (Sigma).

Environmental transcriptome analysis

Two mm inflorescence meristems of *eg1-1*, *eg1-2* and their wild-types ZF802 and ZH11 planted in Beijing summer and Lingshui winter were used for RNA sequencing, and two biological replicates were performed. Total RNAs were isolated with TRIzol kit (Invitrogen). Illumina sequencing libraries were prepared according to the manufacturer's instructions (Illumina Part # 15026495Rev. D), and sequenced with Illumina system Hiseq2500. Analysis of RNA-seq data was conducted following the standard protocol as described by Trapnell et al. [84]. The raw reads of RNA-seq were mapped to MSU_IRGP_V7 (*japonica*) and *Oryza_indica*ASM465 v1.23 (*indica*) by Tophat [85]. Cuffdiff [85,86] was used to identify the differentially expressed genes between different genotypes or different environments. Co-expression network analysis was performed using R packages WGCNA. Enrichment pathways of genes significantly and specifically affected by G, E or GxE was analyzed and the -log10 (P-values) was tested by Fisher's exact test with Bonferroni correction as described by Lu et al. [87].

Evolutionary analysis

Amino acids sequences of EG1 homologs in different plants were aligned with CLUSTAL W and maximum likelihood tree was constructed with MEGA6.0. Subcellular localizations of proteins were predicted with five sorts of software online. Among them, TargetP [88] (<http://www.cbs.dtu.dk/services/TargetP/>) has the best consistency compared with MitoProt II-v1.101 [80] (<https://ihg.gsf.de/ihg/mitoprot.html>), iPSORT [89] (<http://ipsort.hgc.jp/>), ProtComp 9.0 (<http://linux1.softberry.com/berry.phtmtopic=protcompan&group=help&subgroup=proloc>) and WoLF PSORT (<http://www.genscript.com/wolf-psort.html>) online. Predicted localizations with TargetP were shown in our results, a/b in which means the protein is more likely in "a" location than in "b" although both are possible.

Supporting Information

S1 Fig. Variable phenotypes of *eg1-1* and -2. Variable phenotypes of spikelets are defined as [S1 Table](#). le, lemma; pa, palea; eg, empty glume; if, inflorescence primordia; sp, smaller pa; lel, lemma-like organ; pl, palea-lemma mosaic organ; leg, long empty glume in spikelet structures. Bars = 2 mm.

(TIF)

S2 Fig. Mutations of five *eg1* alleles. The predicted full-length CDS (1308 bp) of *EG1* is shown. Horizontal red line indicates the sequence of lipase_3 domain, vertical black lines the mutation locations of alleles, and numbers in the bracket the numbers of bases from “A”.

(TIF)

S3 Fig. Relative expressions of *EG1* in young inflorescences of several *indica* and *japonica* varieties. Values are means ± SE.

(TIF)

S4 Fig. Local and seasonal variations of average daily temperatures during booting stage of rice. High/low temperature (T) per day during rice booting stage. Weather data of summer of Beijing and winter of Lingshui (a), or February and April of Lingshui (b) are shown. Values are means ± SD.

(TIF)

S5 Fig. Co-transformation of *pCAMBIA1301-Pro35S-EG1-GFP* and *MTS-mOrange* in rice protoplasts. Green and red colors indicate the fluorescence of EG1-GFP and MTS-mOrange, respectively. Blue color indicates auto-fluorescence emitted by chloroplasts. DIC, pictures photographed by differential interference contrast microscope. Bar = 10 μm.

(TIF)

S6 Fig. The normal spikelet and seed set rates in *EG1* complementation lines. Normal spikelet rate is the percentage of normal spikelets in a rice panicle, and seed set rate is the percentage of fully grown seeds in a panicle. Values are mean ± SE, number of analyzed panicles = 5.

(TIF)

S7 Fig. Temperature-dependent gene expression of *EG1*. (a) RT-qPCR analysis of *EG1* expression in one-week seedlings of ZF802 and ZH11 wild-types treated under cold shock (4°C) for hours. Values are means ± SE (n = 3), and significant difference was determined by ANOVA, *P < 0.05, **P < 0.01, and rice α -TUBULIN as the reference. (b) RT-qPCR analysis of *EG1* expression in the young inflorescence of ZH11 wild-type treated under extremely high temperature (42°C) for hours. (c) RT-PCR analysis of FLAG-*EG1* expression in one-week seedlings of *EG1* complementation lines treated under different temperatures. Two pairs of FLAG-*EG1* primers and three independent samples were used for analysis. Rice α -TUBULIN was for the reference. (d) Detection of FLAG-*EG1* protein in *EG1* complementation lines at 35°C for 0, 3, or 5 days. HC, Heavy chain of IgG; NS, Nonspecific band (as a loading control). (e) Detection of GFP protein under three temperatures (25°C, 35°C and 42°C) in the *ProUBIQUITIN-GFP* transgenic plants by western blot. RbcL was used as a loading reference. (f) Detection of the peptides derived from FLAG-*EG1* by mass spectrometry. FLAG-*EG1* was purified from one-week seedlings of *EG1* complementation lines and analyzed by MS. The peptides detected are shown in red letters.

(TIF)

S8 Fig. Analysis of *EG1* localization under different temperatures. (a) EG1-GFP localization under normal (28°C) or extremely high (40°C) temperatures in rice protoplasts. Mitochondria

(Mit) and chloroplasts (Chl) are detected by Mito Tacker Red and auto-fluorescence. (b) Fractionation of mitochondria and chloroplasts in EG1 complementation line under different temperatures. Cp, Complementation lines; Ct, non-transgenic wild-type control. CB, Coomassie brilliant blue dyeing.

(TIF)

S9 Fig. Seedling phenotype of eg1 under different temperatures. (a) Phenotypes of six-day-old ZF802 and eg1-1 seedlings. Bar = 1 cm. (b) Statistical analysis of root and shoot phenotypes of eg1-1 and ZF802 seedlings. Values are means \pm SE ($n > 20$). Labelled values are ratios of average value of root length or height of eg1-1 to that of ZF802 in the same condition. Significant difference was determined by ANOVA, * $P < 0.05$, ** $P < 0.01$.

(TIF)

S10 Fig. Correlation analysis of the transcriptomic data and floral phenotypes of eg1. (a) The graph of correlations between gene modules and variable phenotypes. Each color represents a gene module (y axis), and six variable phenotypes are traits (x axis). The deeper colors in the middle squares show stronger correlations between modules and traits with positive correlations in red color and negative in green. Numbers in the boxes are correlation factors and P-values (inside brackets). (b) The network for correlations of gene modules and variable phenotypes. (c) Morphological correlation analysis of six floral variable phenotypes of eg1 alleles. (TIF)

S11 Fig. Comparative and correlation analyses of expressional variations of environmentally responsive genes in eg1 alleles. (a) Comparisons of environmentally responsive transcriptomes between two different genotypes. Each point represents a transcript. x and y axes are values of log2 [ratios of gene expression in Beijing to that in Lingshui] of two genotypes respectively. Dotted lines indicate $y = x$ lines and solid lines are the best fit lines by linear regression. (b) Comparisons of environmentally responsive genes between two eg1 alleles or two wild-types. Values of x and y axes are the same as (a). Points represent wild-type-specific (red), eg1-specific (blue) and shared (green) genes. Dotted lines indicate $y = x$ lines. (c) Triangular scatterplot for distribution of total genes in wild-type and eg1 affected by G, E and GxE. Each dot indicates a gene, and the three vertexes of triangle indicate three factors G, E, GxE respectively. The closer distance between a gene and a vertex means the stronger effect of the factor on the gene.

(TIF)

S12 Fig. Expression patterns of 12 JA associated genes in the environmental transcriptomes. Genes with boldface letters indicate genes with significant variations of expression pattern between eg1 and wild-type. Different colors indicate different samples of Beijing (BJ) and Lingshui (LS). Y axis indicates expression level of genes. Labelled values are log2 [ratios of gene mean expressions in BJ to that in LS] in the corresponding genotypes. “**” labels $|\log_2| > 1$. (TIF)

S13 Fig. Expression patterns of a total of 13 floral identity genes in the environmental transcriptomes. Column diagrams are described as in [S12 Fig.](#) (TIF)

S14 Fig. Maximum likelihood tree and predicted subcellular locations of EG1 and its homologs in different species. Proteins from dicots: *Arabidopsis thaliana* (AtDGL/At1g05800, At2g31690, AtDLAH/At1g30370, AtDSEL/At4g18550, AtDAD1/At2g44810), *Glycine max* (Glyma.08G362700, Glyma.18G299300), *Ricinus communis* (28424.t000001(Rc)) and *Medicago truncatula* (Medtr7g006400); from monocots: *Oryza sativa* (LOC_Os11g19340, LOC_Os11g19290, OsEG1, LOC_Os01g67450, LOC_Os02g42170), *Brachypodium distachyon* (Bradi4g20220,

Bradi4g20230, Bradi2g57760), *Zea mays* (GRMZM2G117627_T0, GRMZM5G812425_T01, GRMZM2G406951_T01), *Sorghum bicolor* (Sobic.005G111400, Sobic.007G187000, Sobic.003G390900, Sobic.003G391000); and moss *Physcomitrella patens* (Phpat.022G001500). Gene IDs come from JGI website. chlo, chloroplast; mito, mitochondria; other, without a chlo/mito targeting peptide.

(TIF)

S1 Table. Description of variable phenotypes of *eg1* alleles.

(XLSX)

S2 Table. Differences of PLACE elements in the 4 kb putative promoters of *EG1* in different genetic backgrounds.

(XLSX)

S3 Table. Temperature-related cis-regulatory elements in the 2kb promoter of *EG1*.

(XLSX)

S4 Table. Genes significantly affected by G, E and GxE in wild-type and *eg1*.

(XLSX)

S5 Table. Genes of thirteen major pathways significantly affected by G, E and GxE in wild-type and *eg1*.

(XLSX)

S6 Table. Predicted subcellular localizations of *EG1* and its homologs with five online softwares.

(XLSX)

S7 Table. Primers for genotyping the mutants.

(XLSX)

S8 Table. Primers for vector constructions.

(XLSX)

S9 Table. Primers for RT-QPCR or RT-PCR.

(XLSX)

Acknowledgments

We thank Dr. Zhukuan Cheng (Institute of Genetics and Developmental Biology, Chinese Academy of Sciences, China) for providing seeds of *gl-ele* and *nsr* mutants, Dr. Yaoguang Liu (South China Agricultural University, China) for plasmids *MTS-mOrange* and *35SPro:COX11-GFP*, and Dr. Dabing Zhang (Shanghai Jiao Tong University, China) for plasmid *pCAM-BIA1301-Pro35S:EG1-GFP*.

Author Contributions

Conceived and designed the experiments: YX WQ. Performed the experiments: BZ YZ TX FG HT XL PW. Analyzed the data: YX BZ SW. Wrote the paper: YX BZ.

References

1. Sultan SE. Plant developmental responses to the environment: eco-devo insights. *Curr Opin Plant Biol.* 2010; 13(1): 96–101. doi: [10.1016/j.pbi.2009.09.021](https://doi.org/10.1016/j.pbi.2009.09.021) PMID: [19857987](https://pubmed.ncbi.nlm.nih.gov/19857987/)
2. Meinzer FC. Functional convergence in plant responses to the environment. *Oecologia.* 2003; 134(1): 1–11. PMID: [12647172](https://pubmed.ncbi.nlm.nih.gov/12647172/)

3. Bradshaw AD. Unravelling phenotypic plasticity—why should we bother? *New Phytol.* 2006; 170(4): 644–648. PMID: [16684227](#)
4. Price TD, Qvarnstrom A, Irwin DE. The role of phenotypic plasticity in driving genetic evolution. *Proc Biol Sci.* 2003; 270(1523): 1433–1440. PMID: [12965006](#)
5. Sultan SE. Evolutionary Implications of Phenotypic Plasticity in Plants. *Evol Biol.* 1987; 21: 127–178.
6. Sultan SE. Phenotypic plasticity and plant adaptation. *Acta Bot Neerl.* 1995; 44(4): 363–383.
7. Bell DL, Sultan SE. Dynamic phenotypic plasticity for root growth in *Polygonum*: A comparative study. *Am J Bot.* 1999; 86(6): 807–819. PMID: [10371723](#)
8. Kembel SW, Cahill JF Jr. Plant phenotypic plasticity belowground: a phylogenetic perspective on root foraging trade-offs. *Am Nat.* 2005; 166(2): 216–230. PMID: [16032575](#)
9. Niinemets U, Valladares F, Ceulemans R. Leaf-level phenotypic variability and plasticity of invasive *Rhododendron ponticum* and non-invasive *Ilex aquifolium* co-occurring at two contrasting European sites. *Plant Cell Environ.* 2003; 26(6): 941–956. PMID: [12803621](#)
10. Yu P, White PJ, Hochholdinger F, Li C. Phenotypic plasticity of the maize root system in response to heterogeneous nitrogen availability. *Planta.* 2014; 240(4): 667–678. doi: [10.1007/s00425-014-2150-y](#) PMID: [25143250](#)
11. Armbruster WS, Di Stilio VS, Tuxill JD, Flores TC, Velasquez Runk JL. Covariance and decoupling of floral and vegetative traits in nine Neotropical plants: a re-evaluation of Berg's correlation-pleiades concept. *Am J Bot.* 1999; 86(1): 39–55. PMID: [21680344](#)
12. Ghaderi A, Lower RL. Heterosis and Phenotypic Stability of F1 Hybrids in Cucumber under Controlled Environment. *J Am Soc Hortic Sci.* 1978; 103(2): 275–278.
13. Kaneko K. Relationship among phenotypic plasticity, phenotypic fluctuations, robustness, and evolvability: Waddington's legacy revisited under the spirit of Einstein. *J Biosciences.* 2009; 34(4): 529–542.
14. Ibanez S, Dujardin G, Despres L. Stability of floral specialization in *Trollius europaeus* in contrasting ecological environments. *J Evol Biol.* 2009; 22(6): 1183–1192. doi: [10.1111/j.1420-9101.2009.01731.x](#) PMID: [19416414](#)
15. Pelabon C, Carlson ML, Hansen TF, Yoccoz NG, Armbruster WS. Consequences of inter-population crosses on developmental stability and canalization of floral traits in *Dalechampia scandens* (Euphorbiaceae). *J Evol Biol.* 2004; 17(1): 19–32. PMID: [15000644](#)
16. Nicotra AB, Atkin OK, Bonser SP, Davidson AM, Finnegan EJ, Mathesius U, et al. Plant phenotypic plasticity in a changing climate. *Trends Plant Sci.* 2010; 15(12): 684–692. doi: [10.1016/j.tplants.2010.09.008](#) PMID: [20970368](#)
17. Smith H. Signal Perception, Differential Expression within Multigene Families and the Molecular-Basis of Phenotypic Plasticity—Introduction. *Plant Cell Environ.* 1990; 13(7): 585–594.
18. Schlichting CD, Wund MA. Phenotypic plasticity and epigenetic marking: an assessment of evidence for genetic accommodation. *Evolution.* 2014; 68(3): 656–672. doi: [10.1111/evo.12348](#) PMID: [24410266](#)
19. Bourdeau PE, Butlin RK, Bronmark C, Edgell TC, Hoverman JT, Hollander J. What can aquatic gastropods tell us about phenotypic plasticity? A review and meta-analysis. *Heredity.* 2015; 115(4): 312–321. doi: [10.1038/hdy.2015.58](#) PMID: [26219231](#)
20. Norouzitallab P, Baruah K, Vandegeehuchte M, Van Stappen G, Catania F, Vanden Bussche J, et al. Environmental heat stress induces epigenetic transgenerational inheritance of robustness in parthenogenetic Artemia model. *FASEB J.* 2014; 28(8): 3552–3563. doi: [10.1096/fj.14-252049](#) PMID: [24755740](#)
21. Oberti D, Biasini A, Kirschmann MA, Genoud C, Stunnenberg R, Shimada Y, et al. *Dicer* and *HSP104* function in a negative feedback loop to confer robustness to environmental stress. *Cell Rep.* 2015; 10(1): 47–61. doi: [10.1016/j.celrep.2014.12.006](#) PMID: [25543137](#)
22. Schlichting CD, Pigliucci M. Control of Phenotypic Plasticity Via Regulatory Genes. *Am Nat.* 1993; 142(2): 366–370. doi: [10.1086/285543](#) PMID: [19425982](#)
23. Pigliucci M. The genetics of plasticity—Reply. *Trends Ecol Evol.* 1996; 11(9): 384–384.
24. Pigliucci M. Modelling phenotypic plasticity.2. Do genetic correlations matter? *Heredity.* 1996; 77: 453–460. PMID: [8939017](#)
25. Soundararajan R, Paranjape AN, Barsan V, Chang JT, Mani SA. A novel embryonic plasticity gene signature that predicts metastatic competence and clinical outcome. *Sci Rep-Uk.* 2015; 5: 11766.
26. Martin-Fairey CA, Nunez AA. Circadian modulation of memory and plasticity gene products in a diurnal species. *Brain Res.* 2014; 1581: 30–39. doi: [10.1016/j.brainres.2014.07.020](#) PMID: [25063362](#)

27. Benito E, Urbanke H, Ramachandran B, Barth J, Halder R, Awasthi A, et al. HDAC inhibitor-dependent transcriptome and memory reinstatement in cognitive decline models. *J Clin Invest.* 2015; 125(9): 3572–3584. doi: [10.1172/JCI79942](https://doi.org/10.1172/JCI79942) PMID: [26280576](https://pubmed.ncbi.nlm.nih.gov/26280576/)
28. Rutherford SL, Lindquist S. HSP90 as a capacitor for morphological evolution. *Nature.* 1998; 396(6709): 336–342. PMID: [9845070](https://pubmed.ncbi.nlm.nih.gov/9845070/)
29. Xu YZ, Santamaria RD, Virdi KS, Arrieta-Montiel MP, Razvi F, Li SQ, et al. The Chloroplast Triggers Developmental Reprogramming When MUTS HOMOLOG1 Is Suppressed in Plants. *Plant Physiol.* 2012; 159(2): 710–720. doi: [10.1104/pp.112.196055](https://doi.org/10.1104/pp.112.196055) PMID: [22496509](https://pubmed.ncbi.nlm.nih.gov/22496509/)
30. Zhang CC, Yuan WY, Zhang QF. RPL1, a Gene Involved in Epigenetic Processes Regulates Phenotypic Plasticity in Rice. *Mol Plant.* 2012; 5(2): 482–493. doi: [10.1093/mp/ssr091](https://doi.org/10.1093/mp/ssr091) PMID: [22131052](https://pubmed.ncbi.nlm.nih.gov/22131052/)
31. Salathia N, Queitsch C. Molecular mechanisms of canalization: HSP90 and beyond. *J Biosciences.* 2007; 32(3): 457–463.
32. Krishna P. Plant HSP90 and its partner proteins. *J Plant Biochem Biot.* 2000; 9(2): 53–56.
33. Queitsch C, Sangster TA, Lindquist S. HSP90 as a capacitor of phenotypic variation. *Nature.* 2002; 417(6889): 618–624. PMID: [12050657](https://pubmed.ncbi.nlm.nih.gov/12050657/)
34. Breiman A. Plant HSP90 and its Co-Chaperones. *Curr Protein Pept Sc.* 2014; 15(3): 232–244.
35. Xu YZ, Arrieta-Montiel MP, Virdi KS, de Paula WBM, Widhalm JR, Basset GJ, et al. MutS HOMOLOG1 Is a Nucleoid Protein That Alters Mitochondrial and Plastid Properties and Plant Response to High Light. *Plant Cell.* 2011; 23(9): 3428–3441. doi: [10.1105/tpc.111.089136](https://doi.org/10.1105/tpc.111.089136) PMID: [21934144](https://pubmed.ncbi.nlm.nih.gov/21934144/)
36. Huang X. A lipid pathway for heat adaptation. *Sci China Life Sci.* 2015; 58(7): 727–728. doi: [10.1007/s11427-015-4880-x](https://doi.org/10.1007/s11427-015-4880-x) PMID: [26044402](https://pubmed.ncbi.nlm.nih.gov/26044402/)
37. Chintalapati S, Kiran MD, Shivaji S. Role of membrane lipid fatty acids in cold adaptation. *Cell Mol Biol (Noisy-le-grand).* 2004; 50(5): 631–642.
38. Zhang YM, Rock CO. Membrane lipid homeostasis in bacteria. *Nat Rev Microbiol.* 2008; 6(3): 222–233. doi: [10.1038/nrmicro1839](https://doi.org/10.1038/nrmicro1839) PMID: [18264115](https://pubmed.ncbi.nlm.nih.gov/18264115/)
39. Strum JC, Ghosh S, Bell RM. Lipid second messengers—A role in cell growth regulation and cell cycle progression. *Adv Exp Med Biol.* 1997; 407: 421–431. PMID: [9321986](https://pubmed.ncbi.nlm.nih.gov/9321986/)
40. Falcone DL, Ogas JP, Somerville CR. Regulation of membrane fatty acid composition by temperature in mutants of *Arabidopsis* with alterations in membrane lipid composition. *BMC Plant Biol.* 2004; 4(1): 1–15.
41. Pan RH, Jones AD, Hu JP. Cardiolipin-Mediated Mitochondrial Dynamics and Stress Response in *Arabidopsis*. *Plant Cell.* 2014; 26(1): 391–409. doi: [10.1105/tpc.113.121095](https://doi.org/10.1105/tpc.113.121095) PMID: [24443516](https://pubmed.ncbi.nlm.nih.gov/24443516/)
42. Chen M, Thelen JJ. ACYL-LIPID DESATURASE2 is required for chilling and freezing tolerance in *Arabidopsis*. *Plant Cell.* 2013; 25(4): 1430–1444. doi: [10.1105/tpc.113.111179](https://doi.org/10.1105/tpc.113.111179) PMID: [23585650](https://pubmed.ncbi.nlm.nih.gov/23585650/)
43. Vamecq J, Dessein AF, Fontaine M, Briand G, Porchet N, Latruffe N, et al. Mitochondrial dysfunction and lipid homeostasis. *Curr Drug Metab.* 2012; 13(10): 1388–1400. PMID: [22978394](https://pubmed.ncbi.nlm.nih.gov/22978394/)
44. Ostrander DB, Zhang M, Mileykovskaya E, Rho M, Dowhan W. Lack of mitochondrial anionic phospholipids causes an inhibition of translation of protein components of the electron transport chain—A yeast genetic model system for the study of anionic phospholipid function in mitochondria. *J Biol Chem.* 2001; 276(27): 25262–25272. PMID: [11335731](https://pubmed.ncbi.nlm.nih.gov/11335731/)
45. Nowicki M, Muller F, Frentzen M. Cardiolipin synthase of *Arabidopsis thaliana*. *Febs Lett.* 2005; 579(10): 2161–2165. PMID: [15811335](https://pubmed.ncbi.nlm.nih.gov/15811335/)
46. Brock MT, Weinig C. Plasticity and environment-specific covariances: an investigation of floral-vegetative and within flower correlations. *Evolution.* 2007; 61(12): 2913–2924. PMID: [17941839](https://pubmed.ncbi.nlm.nih.gov/17941839/)
47. Maier AT, Stehling-Sun S, Wollmann H, Demar M, Hong RL, Haubeiss S, et al. Dual roles of the bZIP transcription factor PERIANTHIA in the control of floral architecture and homeotic gene expression. *Development.* 2009; 136(10): 1613–1620. doi: [10.1242/dev.033647](https://doi.org/10.1242/dev.033647) PMID: [19395639](https://pubmed.ncbi.nlm.nih.gov/19395639/)
48. Sommer H, Beltran JP, Huijser P, Pape H, Lonnig WE, Saedler H, et al. *Deficiens*, a homeotic gene involved in the control of flower morphogenesis in *Antirrhinum majus*: the protein shows homology to transcription factors. *EMBO J.* 1990; 9(3): 605–613. PMID: [1968830](https://pubmed.ncbi.nlm.nih.gov/1968830/)
49. Zachgo S, Silva ED, Motte P, Trobner W, Saedler H, Schwarzsommer Z. Functional-Analysis of the *Antirrhinum* Floral Homeotic *Deficiens* Gene *in vivo* and *in vitro* by Using a Temperature-Sensitive Mutant. *Development.* 1995; 121(9): 2861–2875. PMID: [7555713](https://pubmed.ncbi.nlm.nih.gov/7555713/)
50. Maier AT, Stehling-Sun S, Offenburger SL, Lohmann JU. The bZIP transcription factor PERIANTHIA: a multifunctional hub for meristem control. *Front Plant Sci.* 2011; 2: 79. doi: [10.3389/fpls.2011.00079](https://doi.org/10.3389/fpls.2011.00079) PMID: [22645551](https://pubmed.ncbi.nlm.nih.gov/22645551/)
51. Sablowski RWM, Meyerowitz EM. Temperature-sensitive splicing in the floral homeotic mutant *ape-tala-3-1*. *Plant Cell.* 1998; 10(9): 1453–1463. PMID: [9724692](https://pubmed.ncbi.nlm.nih.gov/9724692/)

52. Yi Y, Jack T. An intragenic suppressor of the Arabidopsis floral organ identity mutant *apetala3-1* functions by suppressing defects in splicing. *Plant Cell*. 1998; 10(9): 1465–1477. PMID: [9724693](#)
53. Li HG, Xue DW, Gao ZY, Yan MX, Xu WY, Xing Z, et al. A putative lipase gene *EXTRA GLUME1* regulates both empty-glume fate and spikelet development in rice. *Plant J*. 2009; 57(4): 593–605. doi: [10.1111/j.1365-313X.2008.03710.x](#) PMID: [18980657](#)
54. Cai Q, Yuan Z, Chen MJ, Yin CS, Luo ZJ, Zhao XX, et al. Jasmonic acid regulates spikelet development in rice. *Nat Commun*. 2014; 5: 3476. doi: [10.1038/ncomms4476](#) PMID: [24647160](#)
55. Ellinger D, Stingl N, Kubigsteltig II, Bals T, Juenger M, Pollmann S, et al. DONGLE and DEFECTIVE IN ANTER DEHISCENCE1 Lipases Are Not Essential for Wound- and Pathogen-Induced Jasmonate Biosynthesis: Redundant Lipases Contribute to Jasmonate Formation. *Plant Physiol*. 2010; 153(1): 114–127. doi: [10.1104/pp.110.155093](#) PMID: [20348210](#)
56. Hyun Y, Choi S, Hwang HJ, Yu J, Nam SJ, Ko J, et al. Cooperation and functional diversification of two closely related galactolipase genes for jasmonate biosynthesis. *Dev Cell*. 2008; 14(2): 183–192. doi: [10.1016/j.devcel.2007.11.010](#) PMID: [18267087](#)
57. Seo YS, Kim EY, Kim WT. The Arabidopsis sn-1-specific mitochondrial acylhydrolase AtDLAH is positively correlated with seed viability. *J Exp Biol*. 2011; 62(15): 5683–5698.
58. Kim EY, Seo YS, Kim WT. AtDSEL, an Arabidopsis cytosolic DAD1-like acylhydrolase, is involved in negative regulation of storage oil mobilization during seedling establishment. *J Plant Physiol*. 2011; 168(14): 1705–1709. doi: [10.1016/j.jplph.2011.03.004](#) PMID: [21477884](#)
59. Padham AK, Hopkins MT, Wang TW, McNamara LM, Lo M, Richardson LGL, et al. Characterization of a plastid triacylglycerol lipase from Arabidopsis. *Plant Physiol*. 2007; 143(3): 1372–1384. PMID: [17259290](#)
60. Luo DP, Xu H, Liu ZL, Guo JX, Li HY, Chen LT, et al. A detrimental mitochondrial-nuclear interaction causes cytoplasmic male sterility in rice. *Nat Genet*. 2013; 45(5): 573–577. doi: [10.1038/ng.2570](#) PMID: [23502780](#)
61. Chen ZX, Wu JG, Ding WN, Chen HM, Wu P, Shi CH. Morphogenesis and molecular basis on *naked seed rice*, a novel homeotic mutation of *OsMADS1* regulating transcript level of AP3 homologue in rice. *Planta*. 2006; 223(5): 882–890. PMID: [16254725](#)
62. Khanday I, Yadav SR, Vijayraghavan U. Rice *LHS1/OsMADS1* controls floret meristem specification by coordinated regulation of transcription factors and hormone signaling pathways. *Plant Physiol*. 2013; 161(4): 1970–1983. doi: [10.1104/pp.112.212423](#) PMID: [23449645](#)
63. Prasad K, Parameswaran S, Vijayraghavan U. OsMADS1, a rice MADS-box factor, controls differentiation of specific cell types in the lemma and palea and is an early-acting regulator of inner floral organs. *Plant J*. 2005; 43(6): 915–928. PMID: [16146529](#)
64. Jeon JS, Lee S, An G. Intragenic control of expression of a rice MADS box gene *OsMADS1*. *Mol Cells*. 2008; 26(5): 474–480. PMID: [18688178](#)
65. Prasad K, Sriram P, Kumar CS, Kushalappa K, Vijayraghavan U. Ectopic expression of rice *OsMADS1* reveals a role in specifying the lemma and palea, grass floral organs analogous to sepals. *Dev Genes Evol*. 2001; 211(6): 281–290. PMID: [11466523](#)
66. Duan Y, Xing Z, Diao Z, Xu W, Li S, Du X, et al. Characterization of *Osmads6-5*, a null allele, reveals that *OsMADS6* is a critical regulator for early flower development in rice (*Oryza sativa* L.). *Plant Mol Biol*. 2012; 80(4–5): 429–442. doi: [10.1007/s11103-012-9958-2](#) PMID: [22933119](#)
67. Zhang J, Nallamilli BR, Mujahid H, Peng Z. *OsMADS6* plays an essential role in endosperm nutrient accumulation and is subject to epigenetic regulation in rice (*Oryza sativa*). *Plant J*. 2010; 64(4): 604–617. doi: [10.1111/j.1365-313X.2010.04354.x](#) PMID: [20822505](#)
68. Ohmori S, Kimizu M, Sugita M, Miyao A, Hirochika H, Uchida E, et al. *MOSAIC FLORAL ORGANS1*, an *AGL6*-like MADS box gene, regulates floral organ identity and meristem fate in rice. *Plant Cell*. 2009; 21(10): 3008–3025. doi: [10.1105/tpc.109.068742](#) PMID: [19820190](#)
69. Li H, Liang W, Jia R, Yin C, Zong J, Kong H, et al. The *AGL6*-like gene *OsMADS6* regulates floral organ and meristem identities in rice. *Cell Res*. 2010; 20(3): 299–313. doi: [10.1038/cr.2009.143](#) PMID: [20038961](#)
70. Gao X, Liang W, Yin C, Ji S, Wang H, Su X, et al. The *SEPALLATA*-like gene *OsMADS34* is required for rice inflorescence and spikelet development. *Plant Physiol*. 2010; 153(2): 728–740. doi: [10.1104/pp.110.156711](#) PMID: [20395452](#)
71. Yoshida A, Suzuki T, Tanaka W, Hirano HY. The homeotic gene *Long Sterile Lemma (G1)* specifies sterile lemma identity in the rice spikelet. *Proc Natl Acad Sci U S A*. 2009; 106(47): 20103–20108. doi: [10.1073/pnas.0907896106](#) PMID: [19901325](#)

72. Hong LL, Qian Q, Zhu KM, Tang D, Huang ZJ, Gao L, et al. *ELE* restrains empty glumes from developing into lemmas. *J Genet Genomics*. 2010; 37(2): 101–115. doi: [10.1016/S1673-8527\(09\)60029-1](https://doi.org/10.1016/S1673-8527(09)60029-1) PMID: [20227044](#)
73. Rudus I, Terai H, Shimizu T, Kojima H, Hattori K, Nishimori Y, et al. Wound-induced expression of *DEFECTIVE IN ANther DEHIScENCE1* and *DAD1*-like lipase genes is mediated by both *CORONAtine INSENSITIVE1*-dependent and independent pathways in *Arabidopsis thaliana*. *Plant Cell Rep.* 2014; 33(6): 849–860. doi: [10.1007/s00299-013-1561-8](https://doi.org/10.1007/s00299-013-1561-8) PMID: [24430866](#)
74. Haluzik M, Colombo C, Gavrilova O, Chua S, Wolf N, Chen M, et al. Genetic background (C57BL/6J versus FVB/N) strongly influences the severity of diabetes and insulin resistance in *ob/ob* mice. *Endocrinology*. 2004; 145(7): 3258–3264. PMID: [15059949](#)
75. Threadgill DW, Dlugosz AA, Hansen LA, Tennenbaum T, Lichti U, Yee D, et al. Targeted disruption of mouse EGF receptor: effect of genetic background on mutant phenotype. *Science*. 1995; 269(5221): 230–234. PMID: [7618084](#)
76. Miao J, Guo D, Zhang J, Huang Q, Qin G, Zhang X, et al. Targeted mutagenesis in rice using CRISPR-Cas system. *Cell Res.* 2013; 23(10): 1233–1236. doi: [10.1038/cr.2013.123](https://doi.org/10.1038/cr.2013.123) PMID: [23999856](#)
77. Shan Q, Wang Y, Li J, Gao C. Genome editing in rice and wheat using the CRISPR/Cas system. *Nat Protoc.* 2014; 9(10): 2395–2410. doi: [10.1038/nprot.2014.157](https://doi.org/10.1038/nprot.2014.157) PMID: [25232936](#)
78. Bart R, Chern M, Park CJ, Bartley L, Ronald PC. A novel system for gene silencing using siRNAs in rice leaf and stem-derived protoplasts. *Plant Methods*. 2006; 2: 13. PMID: [16808845](#)
79. Rodiger A, Baudisch B, Klosgen RB. Simultaneous isolation of intact mitochondria and chloroplasts from a single pulping of plant tissue. *J Plant Physiol.* 2010; 167(8): 620–624. doi: [10.1016/j.jplph.2009.11.013](https://doi.org/10.1016/j.jplph.2009.11.013) PMID: [20045215](#)
80. Claros MG, Vincens P. Computational method to predict mitochondrial imported proteins and their targeting sequences. *Eur J Biochem*. 1996; 241(3): 779–786. PMID: [8944766](#)
81. Seo YS, Kim EY, Kim JH, Kim WT. Enzymatic characterization of class I *DAD1*-like acylhydrolase members targeted to chloroplast in *Arabidopsis*. *FEBS Lett.* 2009; 583(13): 2301–2307. doi: [10.1016/j.febslet.2009.06.021](https://doi.org/10.1016/j.febslet.2009.06.021) PMID: [19527719](#)
82. Seo YS, Kim EY, Mang HG, Kim WT. Heterologous expression, and biochemical and cellular characterization of *CaPLA1* encoding a hot pepper phospholipase A1 homolog. *Plant J.* 2008; 53(6): 895–908. PMID: [18036200](#)
83. Higo K, Ugawa Y, Iwamoto M, Higo H. PLACE: a database of plant cis-acting regulatory DNA elements. *Nucleic Acids Res.* 1998; 26(1): 358–359. PMID: [9399873](#)
84. Trapnell C, Roberts A, Goff L, Pertea G, Kim D, Kelley DR, et al. Differential gene and transcript expression analysis of RNA-seq experiments with TopHat and Cufflinks. *Nat Protoc.* 2012; 7(3): 562–578. doi: [10.1038/nprot.2012.016](https://doi.org/10.1038/nprot.2012.016) PMID: [22383036](#)
85. Trapnell C, Pachter L, Salzberg SL. TopHat: discovering splice junctions with RNA-Seq. *Bioinformatics*. 2009; 25(9): 1105–1111. doi: [10.1093/bioinformatics/btp120](https://doi.org/10.1093/bioinformatics/btp120) PMID: [19289445](#)
86. Trapnell C, Williams BA, Pertea G, Mortazavi A, Kwan G, van Baren MJ, et al. Transcript assembly and quantification by RNA-Seq reveals unannotated transcripts and isoform switching during cell differentiation. *Nat Biotechnol.* 2010; 28(5): 511–515. doi: [10.1038/nbt.1621](https://doi.org/10.1038/nbt.1621) PMID: [20436464](#)
87. Lu ZF, Yu H, Xiong GS, Wang J, Jiao YQ, Liu GF, et al. Genome-Wide Binding Analysis of the Transcription Activator IDEAL PLANT ARCHITECTURE1 Reveals a Complex Network Regulating Rice Plant Architecture. *Plant Cell*. 2013; 25(10): 3743–3759. doi: [10.1105/tpc.113.113639](https://doi.org/10.1105/tpc.113.113639) PMID: [24170127](#)
88. Emanuelsson O, Nielsen H, Brunak S, von Heijne G. Predicting subcellular localization of proteins based on their N-terminal amino acid sequence. *J Mol Biol.* 2000; 300(4): 1005–1016. PMID: [10891285](#)
89. Bannai H, Tamada Y, Maruyama O, Nakai K, Miyano S. Extensive feature detection of N-terminal protein sorting signals. *Bioinformatics*. 2002; 18(2): 298–305. PMID: [11847077](#)